Fully bio-based hydrogels for biomedical applications with controlled drug release attribute

Highlights

This chapter deals with the fabrication of starch-based synthetic monomer-free hydrogels for biomedical applications. This chapter is divided into two sub-chapters. The first sub-section describes a starch/chitosan-based self-cross-linking hydrogel without the inclusion of any synthetic monomer. To obtain the hydrogel, starch was first oxidized under mild conditions to prepare its bialdehydic derivative. Subsequently, the amino group containing polysaccharide, "chitosan" was introduced on the backbone of oxidized starch via a dynamic Schiff-base reaction. The functionalized starch acts as a macro-cross-linker to cross-link with chitosan via Schiff base formation to contribute structural stability and integrity. The introduction of chitosan contributes stimuli-responsive properties and thus pH-sensitive swelling and drug release behavior was obtained. The second sub-chapter includes a starch/agar-based swelling induced mechanically tough hydrogel with controlled drug release ability. The introduction of agar into the hydrogel resulted in agar dose-dependent swelling-induced mechanical strength. Most importantly both hydrogels exhibit prominent cell viability which makes them suitable for biomedical applications.

Parts of this chapter are published as

[1] Sarmah, D., Rather, M. A., Sarkar, A., Mandal, M., Sankaranarayanan, K., and Karak, N. Self-cross-linked starch/chitosan hydrogel as a biocompatible vehicle for controlled release of drug. *International Journal of Biological Macromolecules*, 237:124206, 2023.

[2] Sarmah, D., Borah, M., Mandal, M., and Karak, N. Swelling induced mechanically tough starch–agar based hydrogel as a control release drug vehicle for wound dressing applications. *Journal of Materials Chemistry B*, 11(13):2927-2936, 2023.

Chapter 6A: Self-cross-linked starch/chitosan hydrogel as a biocompatible pH sensitive drug release system

6A.1. Introduction

Chapter 1 gives evidence that hydrogel received immense importance as a potential candidate for biomedical applications due to their inherent hydrophilicity, adequate permeability, biocompatibility, as well as biodegradable nature. However, most of the literature advocates hydrogels are derived using both synthetic and natural starting materials and thus generate a level of toxicity in biomedical fields. Moreover, the hydrogels synthesized in the previous chapters of this thesis are also partially synthetic monomer-based hydrogels. Thus, it is utmost important to develop completely bio-based hydrogel to make them suitable for biomedical applications. To obtain this hydrogel a self cross-linking strategy is applied between oxidized starch (OS) and chitosan. Literature advocates numerous self-cross-linked hydrogel by using various polysaccharides such as guar gum [1], cellulose [2], starch [3], xanthan gum [4], sodium alginate [5], etc. Dialdehyde groups are introduced on the backbone of these polysaccharides and these groups can self-cross-link with nearby hydroxyl groups and amine groups to form cross-linked network structures. For example, Dai et al. synthesized an oxidized guar gum-based self-assembled hydrogel, by taking the advantage of cyclic acetals formed between the periodate oxidized carbonyl groups and the vicinal hydroxyl groups [1]. The synthesized hydrogel exhibited self-healing ability, and a very small amount of $NaIO_4$ is required for the whole process. Moreover, the diadehydic groups can also react with amine groups via Schiff base reaction to form a cross-linked hydrogel. A Schiff base containing hydrogel was prepared by Zhang et al. using glycol, chitosan, and poly(*N*-isopropyl acrylamide)-co-poly(acrylic acid) for biomedical applications [6]. But utilization of synthetic monomers is the main shortcoming of those hydrogels. In 2020, Li et al. synthesized a hyaluronic acid-based self-healing hydrogel using a Schiff base reaction [7]. Thus, Schiff base reactions have wide applicability in hydrogel preparation, but there are limited literature reports available on the critical investigation of the effect of amine group containing moieties on the overall performance of the hydrogel. Therefore, in this work, we have synthesized a tunable drug release system by varying the amine groups containing moiety with respect to the carbonyl groups containing moiety. The change in molar ratio effect the cross-linking density and swelling ability of the hydrogel and these properties are directly

related to the drug release ability. Thus, by varying the amount of reactants, sustained drug release time can be varied and this would help in further medication of hydrogel for biomedical application.

The hydrogel was characterized by using various spectroscopic and analytical techniques, and the antibacterial activity of the entrapped drug for both gram-positive and gram-negative bacteria was analyzed. A proof-of-concept trial was implemented to investigate the feasibility of the hydrogel as a control drug release vehicle for biomedical applications. To achieve this goal the effect of chitosan on the drug release rate was studied at various pH conditions. The main objective of this work is to study the effect of chitosan on OS to judge the suitability of hydrogel as a drug release vehicle.

6A.2. Experimental

6A.2.1. Materials

Tapioca starch was used as the same grade and specifications as discussed in the previous chapters**.**

Chitosan (low molecular weight) with 90% degree of deacetylation was received from SRL, India. It was used to prepare the main backbone of the hydrogel with pH-sensitive ability.

Sodium meta periodate ($NaIO_4$) is an oxidizing agent which is procured from Merck, India. It is a white solid soluble in water. It was used to introduce dialdehydic groups in the starch backbone.

Acetic acid was supplied by Merck, India. A 5% dilute solution of it was used to dissolve chitosan.

Ampicillin sodium salt was purchased from Sigma Aldrich, Germany. It is an antibacterial drug and is used to investigate the sustained drug release study.

Luria-Bertani (LB) is a nutrient media used in biological study. It was purchased from Himedia, India and used in the cell viability study.

Bacterial strains *such as Staphylococcus aureus* (SA) (MTCC 3160), *Bacillus subtilis* (BS) (MTCC 121), and Gram-negative bacteria: *Yersinia enterocolitica* (YE) (MTCC 859) were purchased from Microbial Type Culture Collection, CSIR-Institute of Microbial Technology, Chandigarh, India. Before analysis, the bacterial strains were cultured in LB broth for 24 h on a shaker-incubator under 180 rpm stirring rate at 37 °C.

Sodium dodecyl sulfate (SDS) was obtained from Himedia, India. It is an anionic

surfactant and was used in cytotoxicity study.

Crystal violet is a dye obtained from Himedia, India. It was used to produce violet color of the formazan obtained in cytotoxicity study.

3-(4,5-Dimethylthiazol-2-yl)-2,5-diphenyltetrazolium bromide (MTT) was obtained from Himedia, India. It is used to evaluate cell viability percentage as a function of redox potential.

Human Embryonic kidney cell (HEK 293) was obtained from Sigma Aldrich. It is commonly used cell line commonly in biomedical research due to its reliable growth. Properly grown cells are used to investigate the cytotoxicity study of the synthesized hydrogel.

Dulbecco's modified Eagle's medium, non-essential amino acids, penicillin-streptomycin solution, L-glutamine, foetal bovine serum, and 4-(2- hydroxyethyl)-1-piperazineethanesulfonic acid were purchased from Sigma, Germany. These chemicals are used to determine the cell viability of the hydrogel.

6A.2.2. Methods

6A.2.2.1. Synthesis of the self-cross-linking hydrogel

The OS containing chitosan-based hydrogel was synthesized by following a simple one-pot procedure. Briefly, a calculated amount of tapioca starch was stirred with distilled water in a three neck round bottom flask. The temperature of the starch-water mixture was enhanced up to the formation of a transparent mass and then allowed to cool to 30-35 °C. Then to commence the oxidation of starch, different amounts of $NaIO_4$ (0.05, 0.1, and 0.2 g for 1 g starch) were added, separately, to the reaction mixture in a dark environment up to the formation of a gel-like product. Thereafter the OS produced with the highest amount of $NaIO_4$ was reacted with the desired amount of chitosan powder with a 5 % acetic acid solution. Then the reaction mass was stirred up to the formation of the OS-chitosan gel. Various compositions of the hydrogel were prepared with 0.1 g, 0.2 g, and 0.3 g chitosan and encoded as OSC1, OSC2, and OSC3, respectively. The hydrogels, thus, obtained were washed with distilled water to remove the unreacted substances and subsequently used for encapsulation of the drug for further study.

6A.2.3. Structural analysis

FTIR spectra and XPS analysis were recorded using the same instrument and same

condition as mentioned in **Chapter 2** (Section **2.2.3**).

6A.2.4. Thermal analysis

TGA analysis was recorded using the same instrument and same condition as mentioned in **Chapter 2.**

6A.2.5. Rheological measurements

The rheological measurements of the hydrogels were done on a Rheometer (Anton Paar, Austria, MCR 92) using a plate with a cone angle of 1° and 20 mm diameter with a gap size of 1 mm.

6A.2.6. Swelling test

The swelling study of the synthesized hydrogels was done both in the distilled water and different pH solutions. Calculated amount of hydrogels were immersed in an aqueous medium as described in **Chapter 2**. To determine the swelling ability similar method and mathematical equation was used as described in **Chapter 2.**

6A.2.7. Drug loading in hydrogel

Before loading, the drug was dissolved in distilled water. Pre-weighted hydrogels of all the compositions were taken and the drug solution was added equally to each composition in such a way that the theoretical drug loaded amount was 30% for each sample. Thereafter the drug-loaded hydrogels were dried in a vacuum oven at 50-60 °C. The dry hydrogels were washed with distilled water and the solution was filtered and the aliquots were analyzed using a UV-Vis spectrophotometer (at 227 nm wavelength). The concentration of the drug in the washout water was determined using a calibration curve prepared by using different known concentrations of ampicillin. The encapsulation efficiency of the hydrogel was determined using the following equation.

$$\textbf{Encapsulation efficiency (\%)} = (Q_0-Q_r)/Q_0\times 100 \quad \textbf{---------- Eq. 6A.1}$$

where Q_0 = initial amount of the drug, and Q_r = concentration of the drug in the filtrated solution [8].

6A.2.8. Drug release study

To carry out the controlled release study, the ampicillin-loaded hydrogel was immersed

into 100 mL of different solutions having pH 1.2, 6, and 7.4 under constant stirring. At a particular interval, the buffer samples were collected and concentrations of released ampicillin were determined using a UV-Vis spectrophotometer at the maximum absorption wavelength of the drug. To keep the actual amount of drug release solution constant, the same volume of the aqueous solution was added at same pH as the amount of aliquot was taken out. The concentration of the released drug was determined using a similar method and a calibration curve was used for the determination of the drug release profile. The analysis was performed in triplicate, and the average results were presented with the standard deviation. Cumulative release (%) was calculated as follows.

Cumulative release (%) = $(M_t/M_0) \times 100$ ---------- Eq. 6A.2

where Mt is the amount of drug released from the hydrogel at time t and M_0 is the amount of drug actually loaded onto the hydrogels [9].

6A.2.9. In vitro antimicrobial analysis

Agar well diffusion method was performed to determine the antibacterial activities of the drug loaded hydrogel. Various Gram-positive bacteria such as SA, BS, and Gram-negative bacteria, YE were used to carry out the antibacterial study. An amount of 100 µL each of the overnight bacterial cultures was taken and spread evenly on the surface of LB agar plates. A 6 mm metallic borer was used to make the wells. The drug-loaded hydrogel, hydrogel without drug, and ampicillin solution containing a similar amount to the drug-loaded hydrogel (as positive control) were added to each plate. Subsequently, the plates were incubated at 37 °C overnight. Thereafter, the plates were screened, and the diameters of the zone of inhibition (in mm) were determined [10].

6A.2.10. Cytotoxicity analysis of OSC3 on human embryonic kidney cells (HEK 293)

To culture the human embryonic kidney cells (HEK 293), Dulbecco's Modified Eagle's Medium was used supplemented with 1% penicillin streptomycin solution, 10% foetal bovine serum, 1% non-essential amino acid, 0.05 % L-glutamine, and 0.6 % 4-(2-hydroxyethyl)-1-piperazineethane sulfonic acid. To evaluate the cytotoxicity of OSC3, 1×10^4 220 HEK 293 cells were cultured for 24 h at 37°C and 5% CO_2 in each well of a 96-well plate. Thereafter two different concentrations (1 mg/mL and 5 mg/mL) of OSC3 hydrogel were added without the addition of the drug. An inverted microscope ZEISS,

Model Axio Vert. A1) was used to study the morphology and cell viability, after incubation of 24 h. To determine the cell viability, after incubation the cells were treated with MTT solution at 37 °C for 4 h in an Eppendorf Galaxy 170 cell culture incubator. In the case of metabolically active cells, MTT was converted by mitochondrial dehydrogenases to a dark purple insoluble formazan. Then these formazan samples were treated with denaturing buffer (HCl, SDS, and isopropanol), and the absorbance was examined at 570 nm using a 96-well plate reader (Thermo Scientific Multiskan GO) [11]. The cell viability was evaluated based on the formazan in treated and untreated wells by following the given equation.

Cell viability (%) = [A]/[Ao] ×100 ----------Eq. 6A.3

where [A] is the absorbance of the hydrogel samples and [Ao] is the absorbance of the control [12]

6A.2.11. Biodegradation

Soil burial method was used to investigate the biodegradation of hydrogel. To carry out this experiment OSC3 hydrogel without the addition of the drug was put in a paper cup containing 30 g of soil with 20 mL of water. Then the cups were buried under soil within a depth of 5-7 cm. After a particular time interval, the hydrogel samples were collected from the soil and washed carefully to remove the surface-adhering soil. The percentage weight loss of the hydrogel was determined by using equation described in **Chapter 2** (section **2.2.6.**)

The degraded hydrogel sample was allowed to dry and surface morphology was studied before, and after degradation by using a Scanning Electron Microscope SEM (JSM 6390 LV, Japan).

6A.3. Results and discussion

6A.3.1. Synthesis of the hydrogel

Periodate oxidation was utilized to prepare the self-cross-linked biopolymeric hydrogel as shown in **Scheme 6A.1**. First, carbonyl groups were introduced via selective oxidation of vicinal hydroxyl groups at C-2 and C-3 positions producing a ring-opened structure. This chemical modification technique introduces large numbers of aldehyde groups on the starch backbone. The aldehyde groups thus generated reacted with the nearby

hydroxyl groups to form cyclic acetals or hemiacetals which results in gelation [1, 13-14]. However, the acetic acid solution used to dissolve the chitosan molecule can break up these cyclic acetals and thus free up the carbonyl groups that react with the amine groups of chitosan via Schiff base reaction and forming the imine bonds.

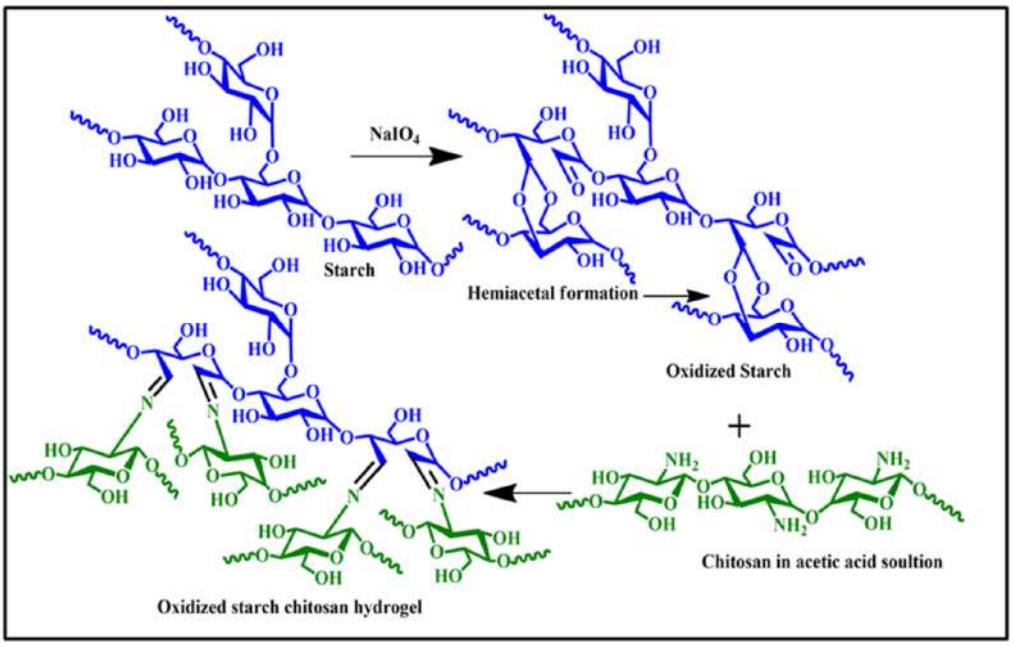

Scheme 6A.1. Possible synthetic route for the preparation of the hydrogel.

Moreover, to certify the oxidation of starch backbone to dialdehydic groups, varying amounts of $NaIO_4$ were allowed to react with the starch. It is seen from **Figure 6A.1.(a** and **b**) that the gelatinized starch (0 g $NaIO_4$) formed with only distilled water was not able to retain its integrity with or without the presence of water.

However, the OS, as obtained with only a very small amount of $NaIO_4$ can retain its integrity in the presence of water and no turbidity was observed instantly, as observed in the case of only gelatinized starch. From the figure, it is clear that the $NaIO_4$ can oxidize starch, and the carbonyl groups thus formed and reacted with the neighboring hydroxyl groups to form the self-assembled hydrogel. The unreacted carbonyl groups react with the nearby amine groups of chitosan to form the Schiff base containing hydrogel. Moreover, in the presence of acetic acid that was used to dissolve chitosan, the cyclic acetals are broken down to form dialdehydic starch and react with the chitosan molecules. The formation of OS/chitosan hydrogel could be evident from **Figure 6A.1. c**. The direct reaction product of the hydrogels also retained their integrity in distilled water as shown in **Figure 6A.1.d**. Thus, this figure gives evidence for the formation of

cross-linking network as the cross-linker is responsible for the retention of the integrity of hydrogel in water.

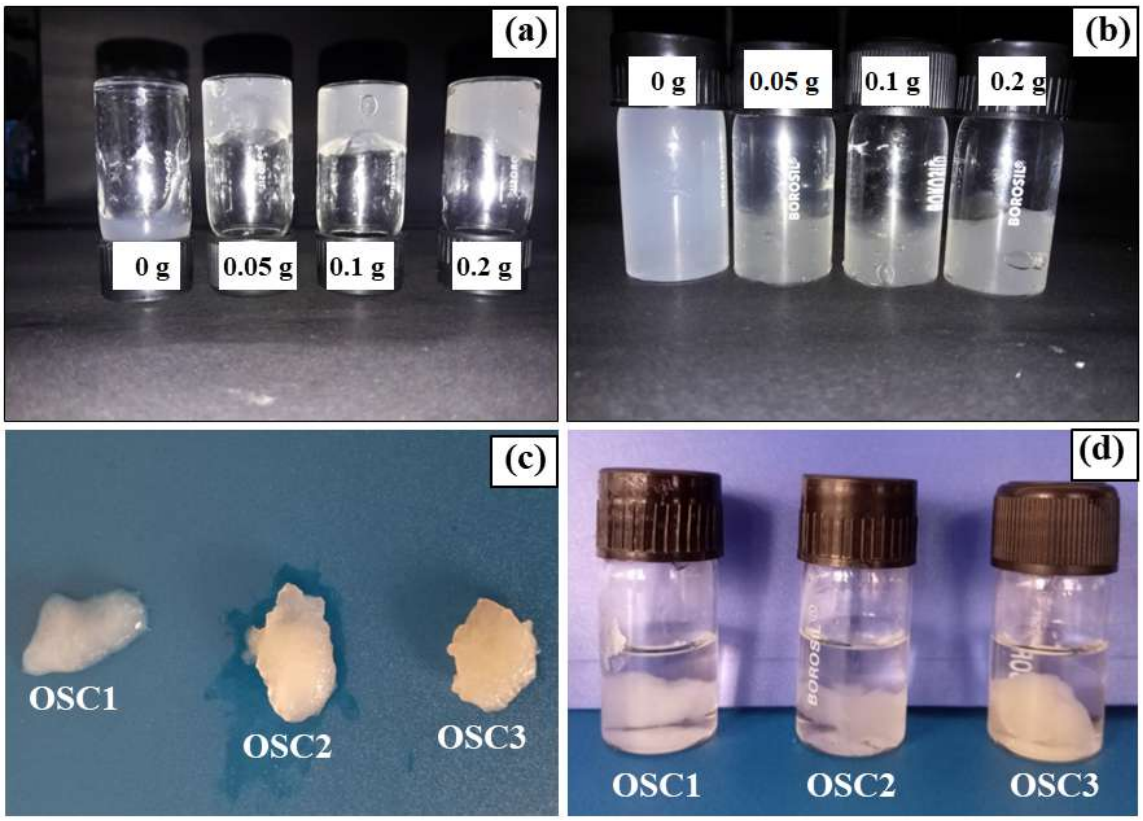

Figure 6A.1. Digital photographs of (a) gelation of OS, as obtained with different amounts of $NaIO_4$, (b) OS in distilled water; (c) hydrogels 'as prepared', and (d) hydrogels in distilled water.

Moreover, to investigate the stability of the synthesized hydrogel we gently put weight on OSC3 hydrogel, as shown in **Figure 6A.2.b**. The breakage of the gel network was not observed under this condition, as shown in **Figure 6A.2.c**. Moreover, all the studied compositions of the dried hydrogel were kept in distilled water and no breakage or turbidity was observed in the water up to 48 h, as shown in **Figure 6A.2.d**. These two phenomena provide enough evidence for the stability of the hydrogels.

6A.3.2. Structural analysis

The structures of the synthesized hydrogels were further confirmed by FTIR, and XPS analyses.

6A.3.2.1. FTIR spectral study

Figure 6A.3.a shows the FTIR spectra of the pristine starch, chitosan, and OS. The FTIR

spectra of the pristine starch and chitosan showed several characteristics bands at 3173.40-3588.21 cm^{-1} and 2818.82-2961.86 cm^{-1} that are associated with the -OH stretching, and symmetric and asymmetric stretching vibrations of C-H groups, respectively [15, 16].

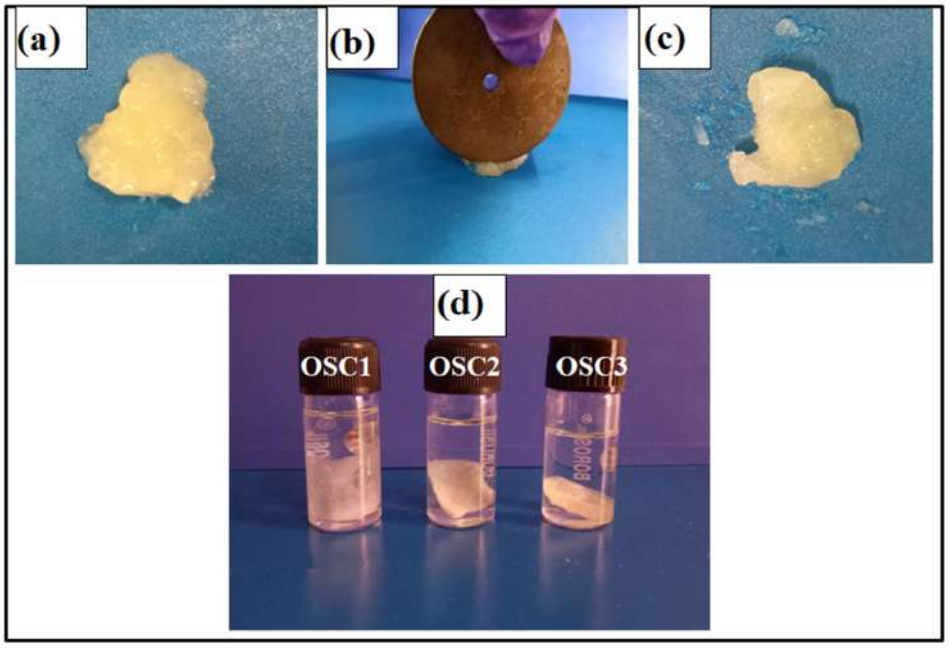

Figure 6A.2. (a) OSC3 hydrogel, (b) OSC3 hydrogel loaded with a weight of 2000 g, (c) OSC3 hydrogel after loading with the given weight, and (d) three hydrogels after keeping for 48 h in water.

In addition to this, the absorption band observed at 1646.94 cm^{-1} and 1599.68 cm^{-1} can be assigned to the stretching vibration of amide I of and NH_2 groups of chitosan, respectively [17]. Moreover, both starch and chitosan contain –C–O–C– stretching vibration at around 1109.15-920 cm^{-1}. After oxidation, the OS displayed a weaker -OH stretching frequency than the pristine one. This signifies the oxidation of starch as well as hemiacetals formation between the carbonyl groups and some of the remaining hydroxyl groups (**Figure 6A.3.a**) [6]. The adsorption band at 1735 cm^{-1} can be attributed to the carbonyl groups formed via the oxidation of starch [18]. But this band is very weak due to the formation of a hemiacetal ring between the carbonyl groups and the free hydroxyl groups [13]. Moreover, the increment of the intensity at 790 cm^{-1} successfully verifies the formation of aldehydic or hemiacetal groups after periodate oxidation.

However, in the FTIR spectra of OS-chitosan hydrogels, the new absorption bands at 1641.04 cm^{-1} and 1570.33 cm^{-1} were observed which can be assigned to the stretching

frequency of amide I and NH_2 of the chitosan side chain (**Figure 6A.3.b**). In addition to this, the band appeared at 1156.48 cm^{-1} due to the –CN stretching frequency of imine groups that are formed by the reaction between the NH_2 groups of chitosan and carbonyl groups of OS [19]. However, the adsorption band at 1735 cm^{-1} observed for OS was not found after the introduction of chitosan. All these facts support the successful formation of imine groups i.e., the Schiff base formation in the hydrogel.

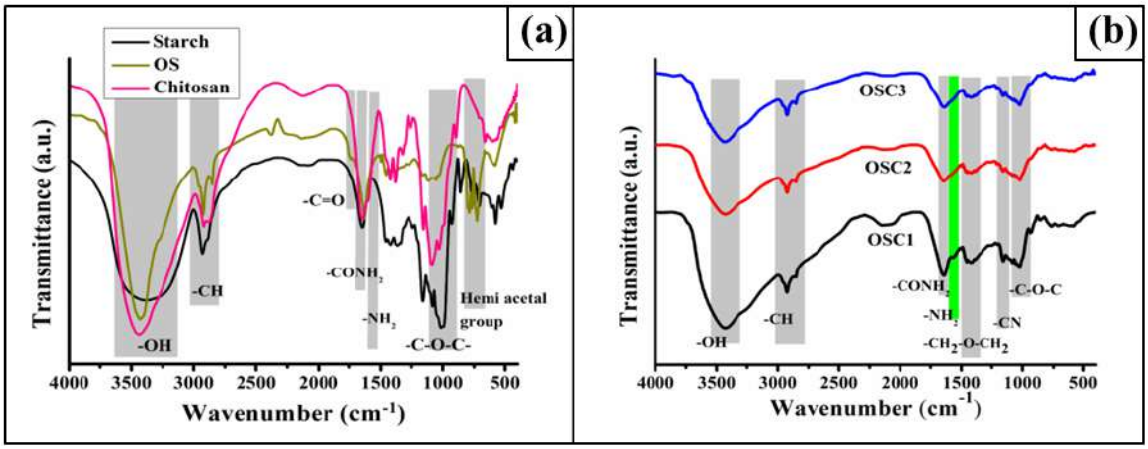

Figure 6A.3. FTIR spectra of (a) starch, chitosan, and OS, and (b) OSC1, OSC2, and OSC3.

6A.3.2.2. XPS analysis

XPS analysis was carried out on OSC3 hydrogel to identify the chemical composition and structure of the hydrogel (**Figure 6A.4.a**). It is found from the analysis that OSC3 contains 59.66% C, 2.16% N, and 38.18% O. The presence of C, O, and N provides evidence of both starch and chitosan in the structure. Further, to understand the chemical state of each atom, a high-resolution XPS analysis was carried out on C 1s, O 1s, and N 1s (**Figure 6A.4.b-d**).

The high-resolution XPS spectrum of C 1s deconvoluted into three peaks at binding energies 320 284.31 eV, 285.57 eV, and 286.26 eV. The peak found at 284.31 eV can be addressed to the C–H and C–C, which constitutes the backbone of both polysaccharides. The second peak observed at slightly higher binding energy represents the C–N carbon atom of chitosan. Moreover, this peak also represents the ether linkage (C–O–C) in the six-member cyclic ring of both starch and chitosan. The third peak found at around 286.26 eV represents the C–O and O–C–O linkages of starch and chitosan backbones. Further, the O 1s spectrum contains one broad peak at around 532.63 eV which can be assigned to C–O and C–O–C groups [20]. Thus, the deconvolution of O 1s also provides

a similar kind of information as found in C 1s. The deconvoluted N 1s peak revealed two different peaks (**Figure 6A.4.d**). The peak at 399.2 eV is attributed to the C–N groups of the nitrogen atom. This can also be attributed to the formation of imine groups in the resulting hydrogel [21]. The second peak at 400.91 eV represents the presence of $–NH_2$ groups and also provides evidence for the presence of chitosan in the hydrogel.

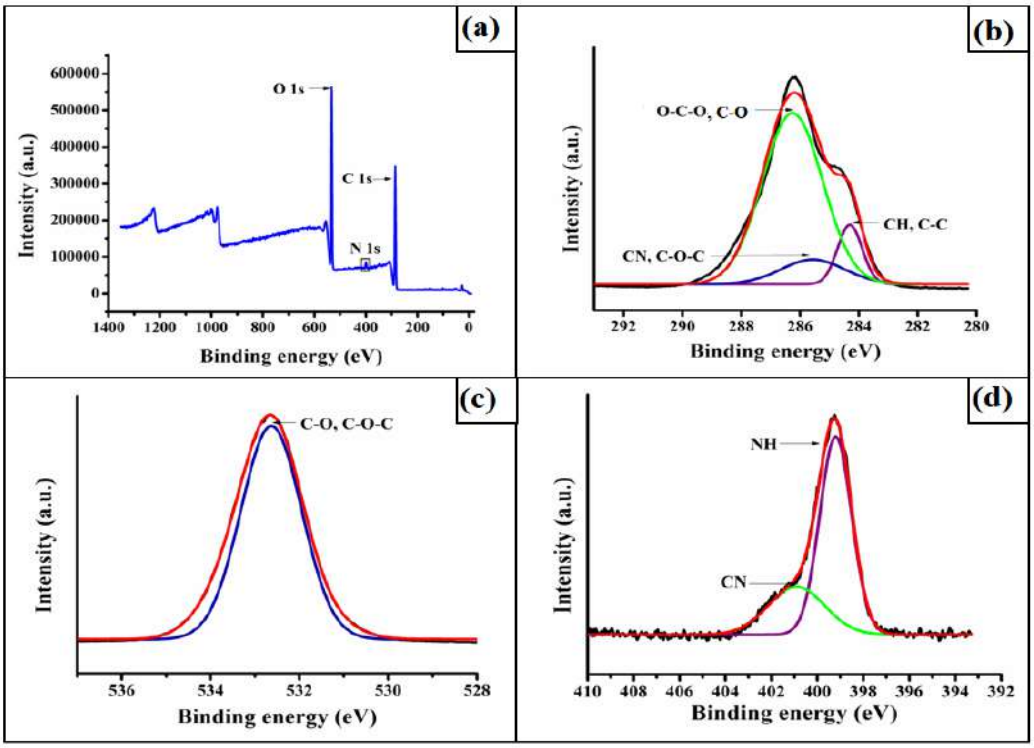

Figure 6A.4. (a) XPS spectra of OSC3, (b) C 1s, (c) O 1s, and (d) N 1s.

6A.3.3. TGA analysis

The thermograms and the first derivatives (DTGs) of pristine starch and chitosan are shown in **Figure 6A.5.**(**a** and **b**). The initial degradation around 70-165 °C is due to the evaporation of water. Polysaccharides usually have a great affinity towards water, and hence they can be easily hydrated [21]. The second weight loss between 312.92 and 344.89 ºC is due to the decomposition of both starch and chitosan backbone [22, 23]. This is a quite complex process that includes the decomposition and depolymerization of monosaccharide rings, and units belonging to starch and chitosan. In the case of OS, the degradation temperature decreases from 337.39 to 317.71 °C indicating their loss in thermal stability. The thermal stability of OS is decreased due to the presence of carbonyl groups and the opening of the six-member ring. The carbonyl groups produced after oxidation is more prone to produce CO, CO_2, and H_2O through thermal degradation [24]. Moreover, after the reaction with chitosan degradation at 282.44 °C was observed.

However, in the case of OSC3 hydrogel also the degradation of both starch and chitosan backbones were observed, as found for the pristine one. From the TGA analysis, it can be concluded that the resulting hydrogel possesses a lower degradation temperature than the pristine starch.

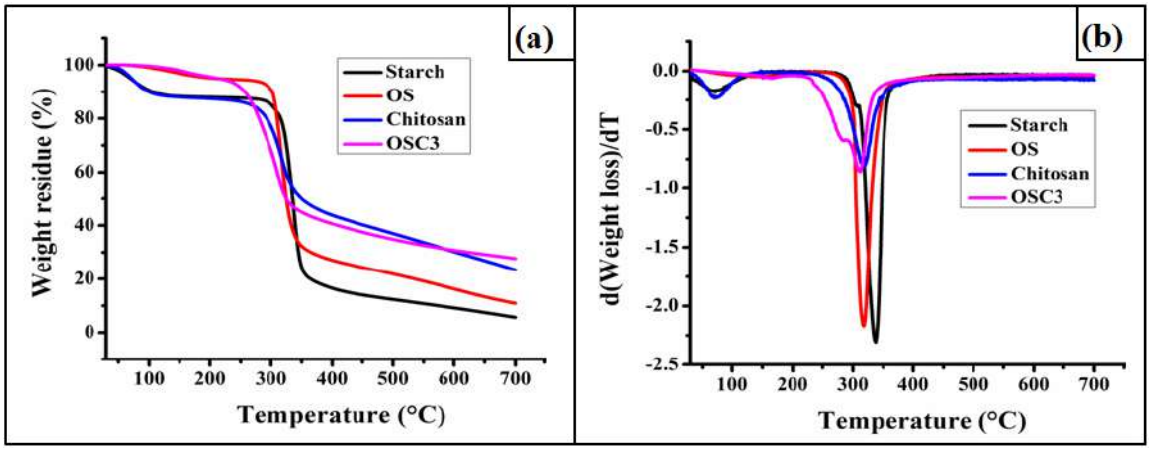

Figure 6A.5. (a) TGA thermograms of starch, OS, chitosan, and OSC3, and (b) first derivative of TG (DTG) of starch, OS, chitosan, and OSC3.

6A.3.4. Rheological study of the hydrogel

The rheological behavior of the synthesized hydrogel was also investigated in all the studied compositions of the hydrogel. To study the influence of cross-linking density i.e., the variation of OS starch and chitosan ratio, a dynamic frequency sweep experiment was carried out. The variations of storage modulus (G') and loss modulus (G") as a function of angular frequency (ω) were carried out for the hydrogels (**Figure 6A.6.a** and **b)**. Higher G' compared to G" over the entire frequency range indicates the solid-like elastic properties of the hydrogels and this gives evidence for the retention of the network structure of the hydrogel during the testing [25]. It is seen that OSC3 hydrogel possesses the highest G′ value compared to the others, followed by OSC2 and OSC1 (**Figure 6A.a**). The hydrogel with the highest chitosan amount is assumed to be exhibited the highest cross-linking density due to the possibility of the highest Schiff base formation. The rheological study provides evidence for this observation and OSC3 hydrogel having the highest chitosan amount, exhibited the highest G' value. This observation was also found by Su et al. in the Schiff base hydrogel formed by using dextran hydrogel containing disulfide bonds [26]. However, in the case of rheological study of G" vs. angular frequency, the order has slightly deviated after a higher angular

frequency value as shown in **Figure 6A.6.b**.

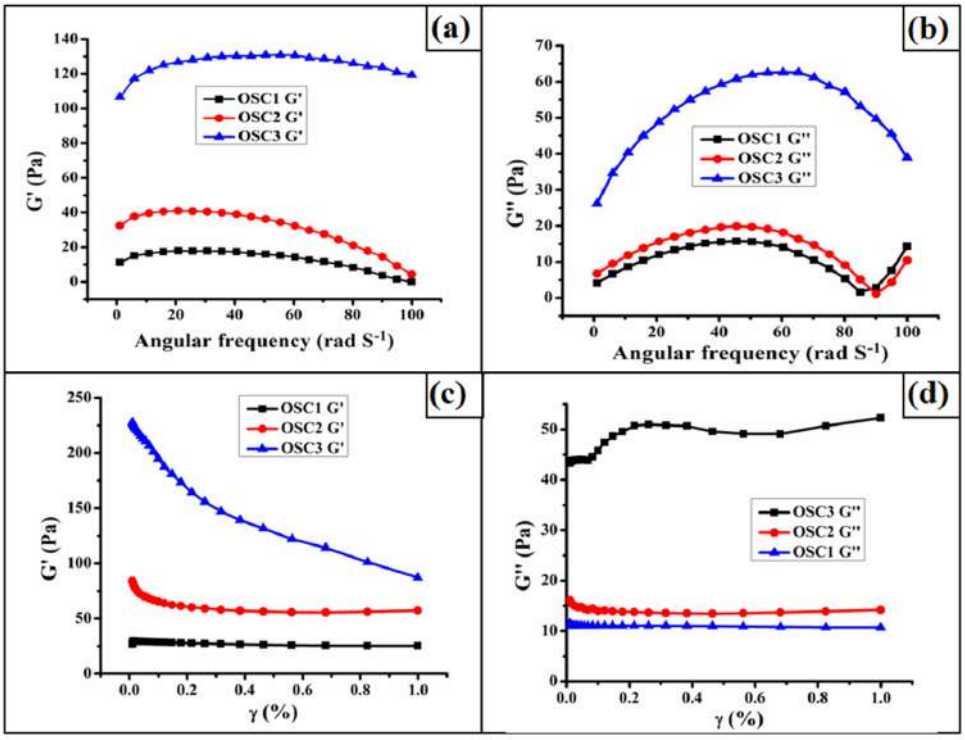

Figure 6A.6. (a) Variation of G' value with angular frequency, (b) variation of G'' value with angular frequency, (c) variation of G' with shear rate, and (d) variation of G'' with shear rate

The viscoelastic behaviors of the synthesized hydrogels were also investigated by strain amplitude sweep method at constant frequency and at 25 ℃. The variation of storage modulus (G') and loss modulus (G'') with shear strain (%) is shown in **Figure 6A.6.(c** and **d**). In all three compositions of the hydrogel, a higher G' value than G'' value indicates that the elastic properties prevailed over the viscous properties of the hydrogels. The G' value decreased with the increase in shear strain value which revealed that there was not any chain entanglement with an increase in shear rate. Moreover, the decrement indicates that there might be the possibility of breaking the gel structure with higher strain. In addition to this, there was not any cross-over between G' and G'' values indicate that the solid-like property of the hydrogel retains intake during the experiment [27]. Moreover, OSC3 exhibited the highest G' and G'' values followed by OSC2 and OSC1. This observation provides evidence for the highest cross-linking density of OSC3 compared to the others. Thus, from this rheological study, it is also confirmed that an increase in the chitosan amount enhanced the possibility of cross-linking inside the hydrogel [27].

6A.3.5. Swelling ability

Swelling is one of the most vital properties for drug release ability and other biomedical applications. The swelling ability of hydrogel depends upon the ionizable or protonated functional groups, the presence of hydrophilic groups, and the relaxation of the polymeric chains [28]. **Figure 6A.7.a** depicts the swelling ability of the hydrogels. The swelling ability was studied in distilled water and at different pH conditions. It is seen that with the increase in the chitosan to starch ratio, a gradual decrease in swelling ability was observed. This phenomenon can be attributed to the cross-linked structure formation, which is related to the amount of Schiff-base generation [29]. The swelling results of the hydrogels under different pH conditions are shown in **Figure 6A.7.b.** The highest swelling was observed in pH 1.2 medium for all the studied compositions and swelling ability decreased with the increase in pH of the solution. This distinctive swelling ability is due to the unique chemical structure of chitosan that possesses one amine group in most of the repeating structural units. In an acidic environment, these amino groups are protonated and generate a higher proton concentration within the hydrogel network than in the surrounding environment. Due to this concentration gradient, there is an osmotic pressure difference inside and outside the gel resulting in higher water flow inside the hydrogel. In addition to this, the protonated amine (NH_3^+) groups act as cationic repulsive forces inside the polymeric membrane leading to a higher swelling ability [29,30]. Moreover, among the three hydrogels, OSC3 exhibited the highest swelling ability at pH 1.2. This is due to a higher amount of chitosan that is present in the hydrogel network which leads to higher repulsion resulting in higher space for the accommodation of a large amount of water molecules inside the three-dimensional network of the gel.

In the basic condition, deprotonation occurs leading to lower swelling ability. Thus, at pH 6 and 7.4 much lower swelling ability was observed compared to pH 1.2. Moreover, the swelling ability of the hydrogel at higher pH followed a similar trend as found in normal distilled water. Thus, OSC1 exhibited the highest swelling ability followed by OSC2 and OSC3. At pH 7.4 due to the absence of protonated groups, cross-linking density dominates the swelling ability, and hence OSC3 having the highest cross-linking density exhibited the lowest swelling degree. Moreover, at pH 6, due to the presence of insufficient amount of H^+ ions, a lower amount of protonation occurs and hence, the cross-linking density predominated the swelling capacity leading to the highest swelling

in the case of OSC1 as shown in **Figure 6A.7.b**.

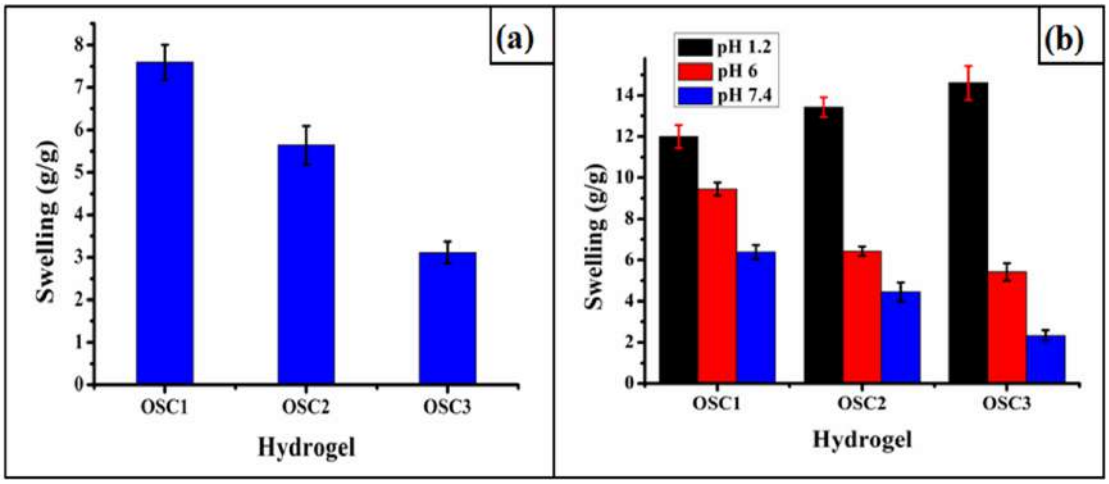

Figure 6A.7. (a) Swelling capacities of the hydrogels in distilled water, and (b) swelling capacities of the hydrogels at different pH conditions.

6A.3.6. Encapsulation efficiency

Encapsulation efficiency is the actual fraction or percentage of drug loaded in the drug encapsulated hydrogel. It is one of the most important parameters for the formation of hydrogel for a sustained drug release system [31]. The percentage encapsulation efficiency of the hydrogel varied from 85.22±0.99% to 90.66±0.85%, as shown in **Figure 6A.8.a**, with the increase in the amount of chitosan in the hydrogel network. The lower encapsulation efficiency with a lower amount of chitosan can be explained due to the formation of a comparatively loose hydrogel structure. The amount of chitosan affects the cross-linking density of the hydrogel and thus, the drug loading amount. A higher cross-linking density was achieved with the increase in chitosan amount which was also observed in the swelling ability of the hydrogels. A hydrogel with higher cross-linking density formed a more rigid structure reducing the possibility of leaching of the drug molecules from the matrix [32].

6A.3.7. In vitro drug release

When a drug containing hydrogel comes in contact with an aqueous medium or body fluid, water penetrates in the system and dissolves the drug molecules. Then the drug molecules come out from the delivery system due to Brownian motions and the concentration gradient of drug molecules [33]. Usually, from a swellable system drug molecules release through diffusion or degradation or sometimes via both the

mechanisms, depending on the swelling degree, the solubility of the drug, and the strength of the gel network [33]. However, in the case of a water-soluble drug, diffusion is the primary mechanism for drug release. Moreover, drug release is greatly affected by the stimuli-responsive property of the delivery system and this property can be used for tuning the release rate at the targeted site. As the hydrogel obtained from this work exhibited pH-sensitive swelling ability, this property was utilized to evaluate the drug release profile, and the optimum release rate was observed under the suitable environmental conditions.

6A.3.7.1. Effect of pH on drug release

To investigate the effect of pH on the drug release rate, we considered different pH conditions (1.2, 6, and 7.4) to release the ampicillin drug from all the hydrogels. The hydrogels exhibited different release rates and release percentages, which depend on the swelling ability of the hydrogel in that particular aqueous solution. The cumulative release profiles of the drug from the hydrogels at different pH conditions are shown in **Figure 6A.8.b-d**. The results indicate that pH plays a key role in the release profile and at pH 1.2, a high amount of drug was released from all the hydrogels. The highest release rate in this pH condition can be attributed to the highest swelling ability of the hydrogel. A hydrogel with high swelling ability can highly expand its three-dimensional network resulting in a comparatively loose network. These phenomena facilitate the diffusion of large numbers of entrapped molecules from the hydrogel network. However, all the studied compositions exhibited the almost same amount of drug at this pH condition, as shown in **Figure 6A.8.b-d**.

However, with an increase in pH from acidic to alkaline, the percentage of drug released was decreased and the release time was increased. Prolonged release time was observed in the case of alkaline medium and follows the order of pH 7.4 > pH 6 > pH 1.2. Shi et al. also investigated the effect of pH on drug release and found a much higher release percentage at pH 6 compared to pH 7.4. However, in our studied system at pH 6, 84.23± 2.19% drug was released from OSC1, within 20 h and thereafter remains almost constant. In the case of OSC2 and OSC3, the release percentage was found to be decreased with the increase in release time, as shown in **Figure 6A.8.b-d**.

At pH 7.4, the hydrogels exhibited similar trends, and OSC3 exhibited a more extended-release profile than OSC2 and OSC1. Thus, these results showed that at high pH, the

release performance is greatly affected by the amount of chitosan i.e., the cross-linking density of the hydrogel. With the increase in chitosan amount, the cross-linking density was increased which affect the swelling ability and thus the drug release rate. At pH 7.4, the drug release performance is controlled by the cross-linking density of the hydrogel, and thus, OSC3 having a highly cross-linked network exhibited the highest sustained release time compared to the others. A similar effect was also observed by Gull et al. in their drug delivery system where hydrogel with higher cross-linking density showed lower drug release ability [31].

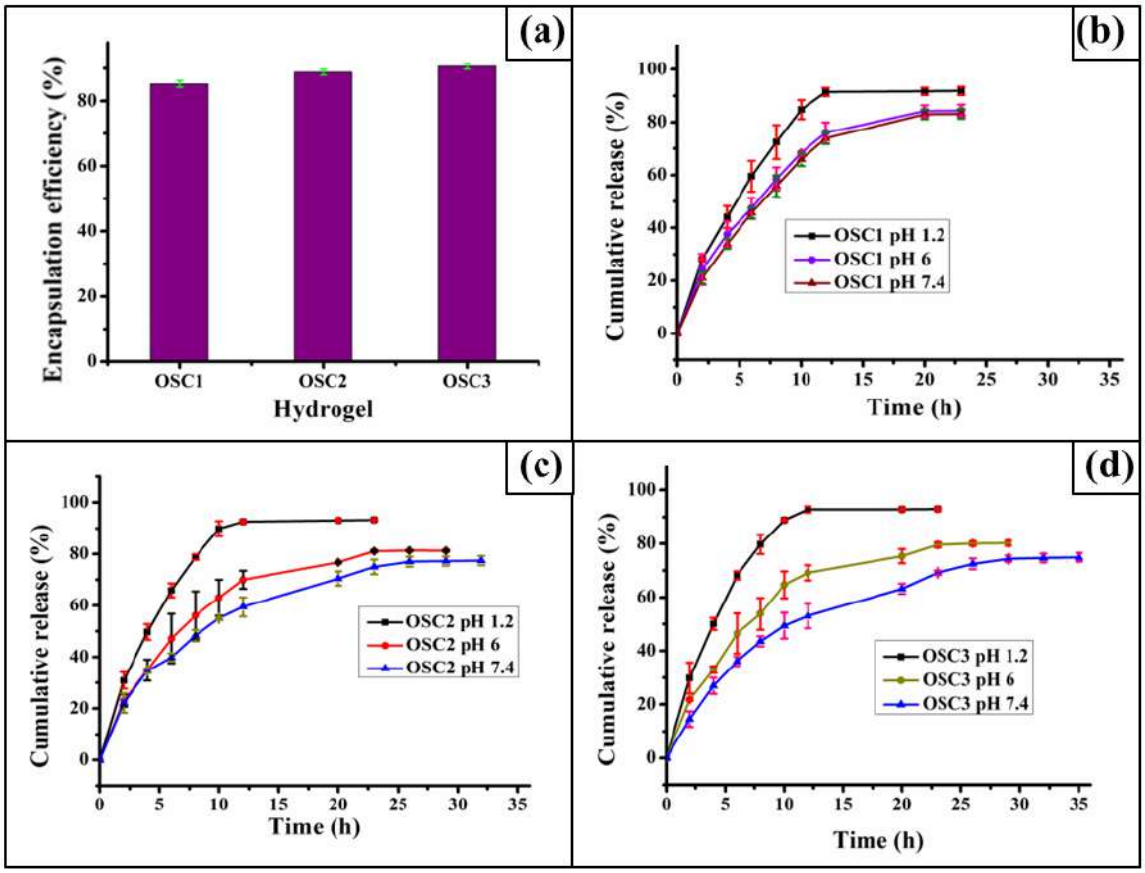

Figure 6A.8. (a) Drug encapsulation efficiency of the hydrogels, and cumulative drug release profile at different pH conditions of (b) OSC1, (c) OSC2, and (d) OSC3.

While, in the case of highly acidic pH, the swelling ability of OSC3 is higher than the other two hydrogels due to the presence of pH-sensitive groups in the chitosan network, which affects the swelling rate and thus the release performance. Hence, in the case of OSC3 hydrogel, almost the same release percentage was observed. While at pH 7.4, OSC3 exhibited the lowest swelling value among the three hydrogels, hence it showed the lowest drug release ability. These results indicate that the release performance is controlled by swelling. Thus, with the altering amount of the starch to chitosan ratio, the

drug release performance can be varied, and hence a tunable release system can be achieved for the targeted site.

6A.3.7.2. Drug release kinetics

Kinetics models play a vital role to investigate the drug release mechanism and intermolecular interaction between drug molecules and the delivery system. Usually, Korsmeyer and Peppas equation is used to analyze the drug release from a swellable system. The mathematical expression of this model is as follows.

$$M_t/M_e = Kt^n \text{ ----------Eq. 6A.4}$$

where M_t and M_e are the drug release at time t and at equilibrium conditions, respectively. K is a constant and n is the diffusion exponent which determines the diffusion mechanism [34]. The plots obtained from ln (M_t/M_e) versus ln t are shown in **Figure 6A.9.(a-c)** for all the compositions at different pH conditions and the values are tabulated in **Table 6A.1**. The value of n obtained from this is used to determine the release mechanism. If n<0.45, then drug release occurs through Fickian diffusion, and the diffusion process plays a predominant role. The value of n between 0.45 to 0.85 indicates non-Fickian diffusion when both diffusion and swelling processes control the overall release rate of the drug [53]. In this study, all the values of n are between 0.45 to 0.85 indicating that the drug release from the hydrogel network occurs through both swelling and diffusion. During swelling, water molecules dissolve the drug and hence easily come out from the pores and outer surface of the gel to the surrounding liquid medium through diffusion.

Moreover, zero order (**Eq. 6A.5**) [35], pseudo first order (**Eq. 6A.6**) [36], and Higuchi square root law (**Eq. 6A.7**) [35, 37] are also used to investigate the drug release mechanism as given below.

$$\mathbf{Mt = M_0 + k_0t} \text{ ---------- Eq. 6A.5}$$

$$\mathbf{\log (M_e - M_t) = -k_1/2.303t + \log M_e} \text{ ---------- Eq. 6A.6}$$

$$\mathbf{M_t = k_2t^{1/2}} \text{ ---------- Eq. 6A.7}$$

where "M_t" and "M_e" are the drug release at different times (t) and at equilibrium conditions, respectively, and k_0, k_1, k_2 are the rate constants.

The data obtained from these kinetics models are shown in **Figure 6A.9.d-6A.10.f** and the correlation factors obtained are given in **Table 6A.1**. All the drug release systems followed Higuchi law with higher correlation factors compared to the other two.

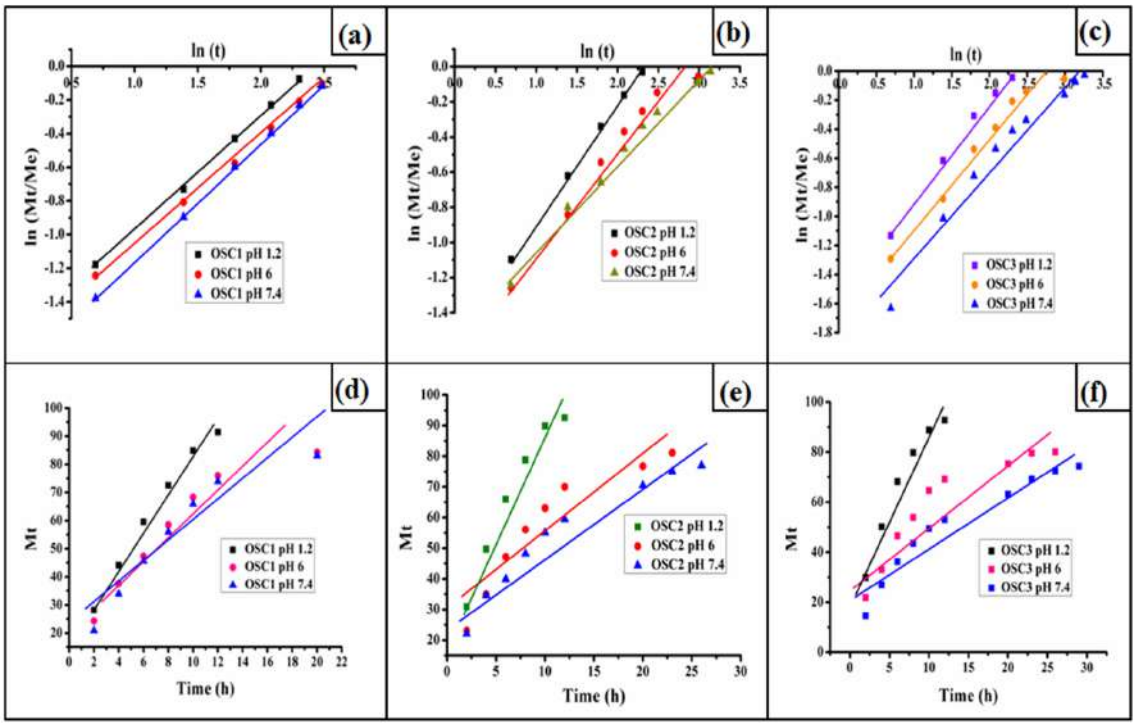

Figure 6A.9. Korsmeyer and Peppas power law for (a) OSC1, (b) OSC2, (c) OSC3; and zero order kinetics for (d) OSC1, (e) OSC2, and (f) OSC3.

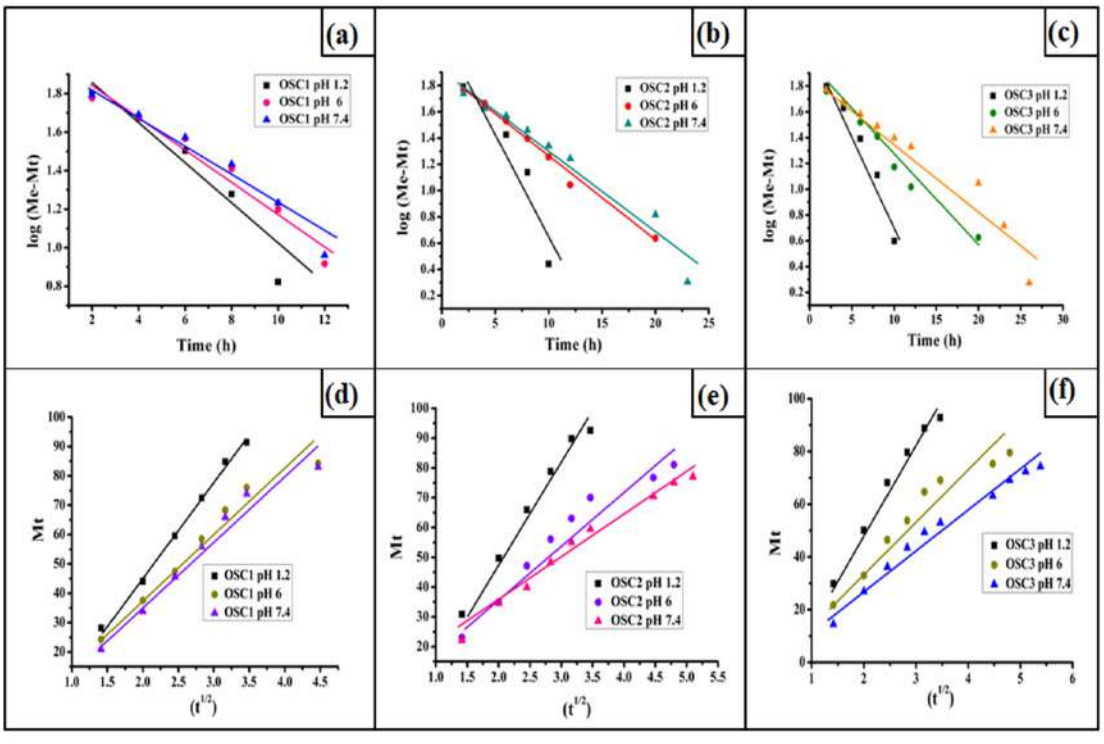

Figure 6A.10. Pseudo first order kinetics for (a) OSC1, (b) OSC2, (c) OSC3; and Higuchi square root law for (d) OSC1, (e) OSC2, and (f) OSC3.

Table 6A.1. Kinetics parameters for drug release systems

Drug release system/pH	Korsmeyer and Peppas power law		Zero-order (R^2)	Pseudo-first order (R^2)	Higuchi square root law (R^2)
	R^2	n value			
OSC1/pH 1.2	0.9990	0.687	0.9812	0.9098	0.9959
OSC1/pH 6	0. 9986	0.64	0.8470	0.9486	0.9477
OSC1/pH 7.4	0.9998	0.71	0.8541	0.9541	0.9528
OSC2/pH 1.2	0.9989	0.67	0.9458	0.8694	0.9862
OSC2/pH 6	0.9635	0.56	0.8292	0.9889	0.9356
OSC2/pH 7.4	0.9844	0.49	0.9113	0.9516	0.9795
OSC3/pH 1.2	0.9922	0.69	0.9304	0.9388	0.9816
OSC3/pH 6	0.9545	0.58	0.8020	0.9785	0.9188
OSC3/pH 7.4	0.9591	0.59	0.9030	0.9361	0.9746

6A.3.8. Antibacterial study

Agar well diffusion method was performed on drug encapsulated OSC3 hydrogel to investigate the antibacterial activity and the results are shown in **Figure 6A.11.**(**a-c**). For better understanding each plate is divided into three segments containing ampicillin solution as the standard, OSC3 without drug, and OSC3 loaded with ampicillin. It is clearly evident from the diameter of the inhibition zone that the plain hydrogel was unable to show any inhibition effect against the tested gram positive and gram-negative bacterial strains. However, the ampicillin-loaded hydrogel exhibited noteworthy antimicrobial activity against the tested bacterial strains. These obtained data confirmed that the drug was successfully loaded on the prepared hydrogel and can release the same. The released ampicillin from the hydrogel can makes the inhibition effect on gram-positive and gram-negative bacterial strains and thus, a noticeable amount of inhibition zone was observed in each case. The diameters of the inhibition zones obtained after exposure to the prepared hydrogel and the control for the gram-positive bacteria (SA, and BS) and the gram-negative bacteria (YE) are provided in **Table 6A.2**. These results indicate that the drug-loaded hydrogel can exhibit its inhibition effect for the bacterial strain and can be used as an antibacterial drug release vehicle.

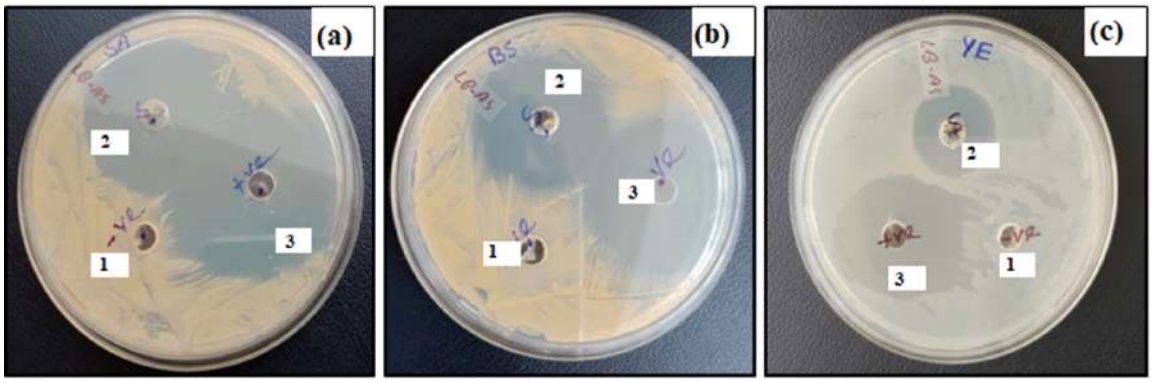

Figure 6A.11. Antimicrobial activity of (1) hydrogel without drug, (2) drug-loaded hydrogel, and (3) control, against (a) SA, (b) BS, and (c) YE.

Table 6A.2. Diameter of inhibition zone of the antibacterial test.

Bacterial strain	Inhibition diameter of hydrogel without drug (mm)	Inhibition diameter of hydrogel with drug (mm)	Inhibition diameter of drug (mm)
SA	0	35.33±1.53	39±0
BS	0	30.67±0.58	34.67±0.58
YE	0	22.33±0.58	29.33±1.15

6A.3.9. Cytotoxicity (cell compatibility) assay

Toxicity of polymeric materials is one of the shortcomings in creating a vehicle for a drug delivery system. To define as a safe drug carrier, the matrix must possess low or no toxicity [38]. The cytotoxicity of OSC3 hydrogel without any drug was tested against Human Embryonic kidney cells (HEK 293) by cell morphology study and MTT assay. The cell was cultured with different concentrations of the tested hydrogel. After 24 h, the cell viability percentage was determined and plotted against the concentration of OSC3 hydrogel (**Figure 6A.12.a**). The numbers of viable cells are directly proportional to the absorbance of MTT at 570 nm [21]. The results revealed that the hydrogel possesses an excellent cell viability percentage at the concentration of 1 mg/mL and 5 mg/mL (**Figure 6A.12.a**). Moreover, the changes in cell morphology were studied by using an inverted microscope, as shown in **Figure 6A.12.(b-d)**. It is seen that there were no visible morphological changes after the treatment with OSC3 hydrogel for 24 h. These results reveal that the prepared hydrogel possesses noteworthy biocompatibility and hence can be considered as a nontoxic controlled drug delivery system.

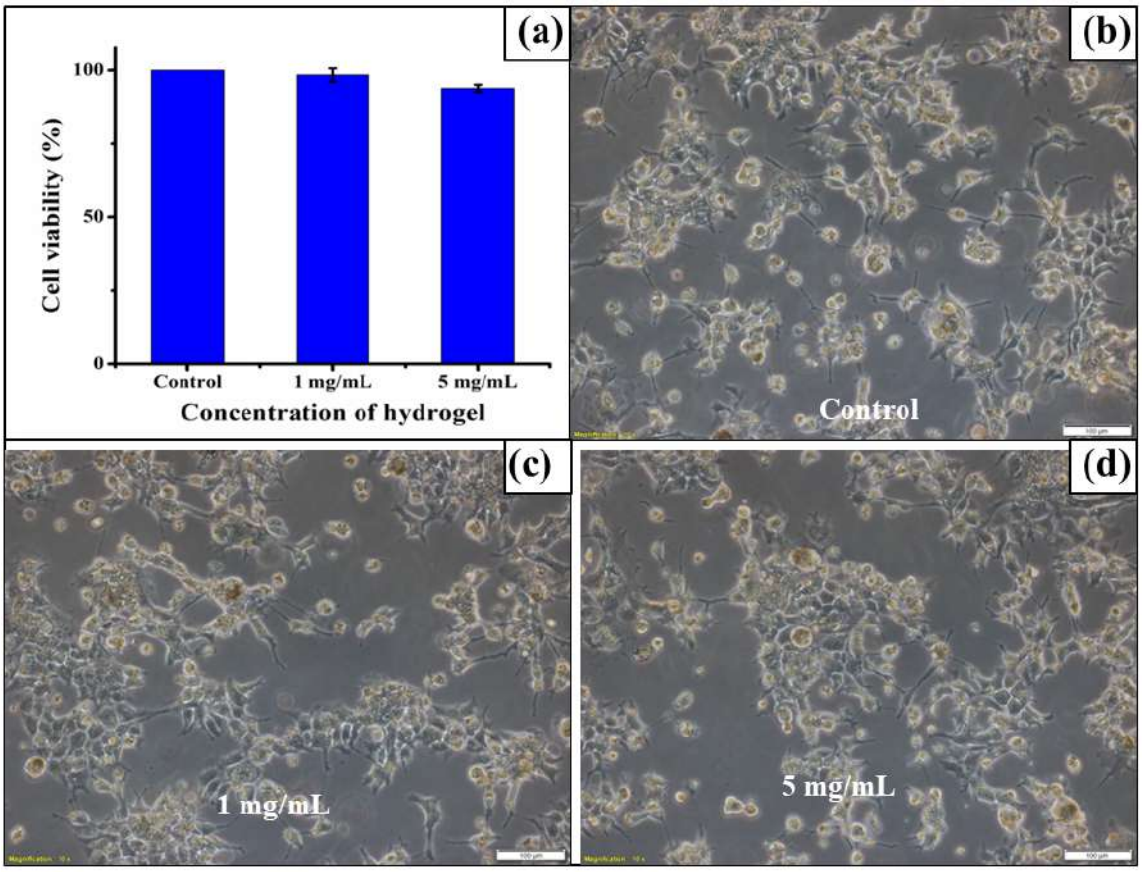

Figure 6A.12. (a) Cell viability of Human Embryonic Kidney cells (HEK 293) upon treatment with OSC3; microscopic images of the cells (b) control, (c) treated with1 mg/mL OSC3, and (d) treated with 5 mg/mL OSC3.

6A.3.10. Biodegradation

Biodegradation of polymeric products is one of the most important qualities to judge them as environmentally friendly materials. The oven dried OSC3 hydrogel without any drug was completely biodegraded in the soil after 15 days and no residue was observed under the soil. The weight loss of the hydrogel after biodegradation under the soil is shown in **Figure 6A.13.a**. Due to the absence of any cross-linker and synthetic monomer, the hydrogels were degraded easily by the microorganism present in the soil [39]. Moreover, to provide evidence for the biodegradation of the hydrogel, SEM images of the non-biodegraded and the biodegraded OSC3 hydrogels were taken as shown in **Figure 6A.13.(b-d)**. For this purpose, the hydrogel before complete degradation was removed from the soil. It is seen that after degradation the surface morphology is completely changed. The surface of the oven dried OSC3 was smooth, and no pore was observed because of the drying process as chain entanglement occurs due to heating.

However, after biodegradation, surface erosion occurred, and the smoothness completely vanished, as shown in **Figure 6A.13.(c-d)**. Thus, SEM analysis gives evidence for the biodegradation of the hydrogel under soil-buried conditions.

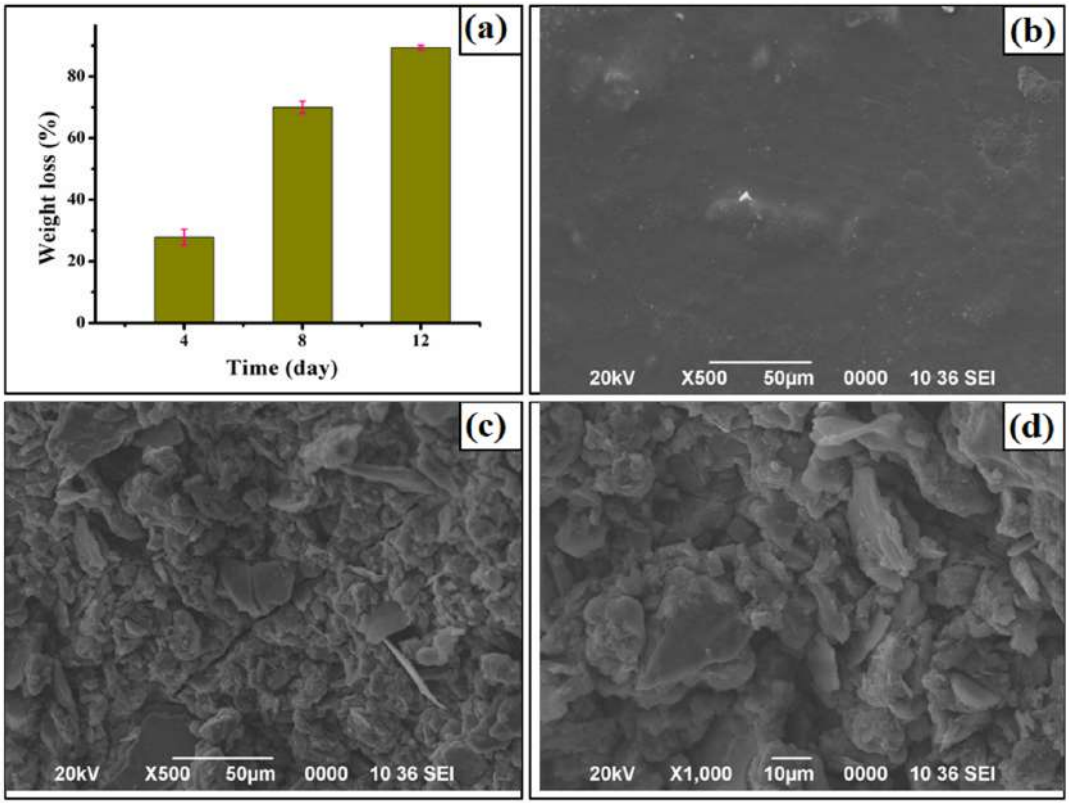

Figure 6A.13. (a) Weight loss with time of the hydrogel upon biodegradation, (b) oven dried OSC3 before biodegradation, and (c-d) OSC3 after biodegradation.

6A.4. Conclusion

In conclusion, this study provides a facile, cross-linker-free, one-pot procedure for the preparation of a polysaccharides-based hydrogel. The hydrogel was characterized by using FTIR, XPS, and TGA analyses and applied as a sustained drug delivery vehicle. The drug entrapment efficiency enhances with the increase in the amount of chitosan in the hydrogel network, and the maximum encapsulation efficiency of 90.66% was observed. The hydrogel showed pH-dependent swelling ability, and the controlled release ability was also affected by the pH of the medium. From the study it is clearly evident that the pH-dependent response of the hydrogel is due to the presence of chitosan in the matrix and varied with the varying amount of chitosan. In vitro study showed that the higher release percentage was observed at pH 1.2. However, the hydrogel exhibited the highest sustained release ability of 29 h at pH 7.4. The kinetics study proved that the

drug release from the hydrogel followed the non-Fickian diffusion model. The ampicillin-loaded hydrogel was effective for various bacterial strains, and a noticeable amount of inhibition zone was achieved. MTT assay of the synthesized hydrogel showed more than 93% cell viability even at concentration of 5 mg/mL. Thus, the prepared hydrogel has great potential as a promising controlled drug delivery vehicle.

Chapter 6B: Swelling induced mechanically tough starch/agar-based hydrogel for wound dressing applications

6B.1. Introduction

Chapter 6A demonstrated pH sensitive oral drug delivery system using a self-cross-linking strategey. However, some of the biomedical applications demand mechanical stability of the biomaterials. Thus, this chapter introduce a mechanically tough starch/agar based hydrogel for wound dressing application. However, over the last few decades, a number of studies have reported mechanically tough hydrogels for dressing applications. For example, in 2017, a pH responsive tough hydrogel was synthesized as a smart dressing material by Liu et al. The hydrogel was synthesized by using sodium alginate, and acryl amide was used as a synthetic monomer [40]. In 2020, a highly stretchable mechanically tough poly(sulfobetaine methacrylate) hydrogel was synthesized by Fang et al [41]. The mechanoresponsive hydrogel showed good adhesive properties, exhibiting 1.41 MPa compressive stress. Recently, a highly stretchable hydrogel was also synthesized using acrylamide as a monomer and *N, N*-bis(acryloyl)cysteamine as the cross-linking agent [42]. Although all these hydrogels have shown potential as effective mechanically tough dressing materials, the use of synthetic monomers limits their applicability. Thus, in this work we aimed to synthesize a polysaccharide-based synthetic monomer-free hydrogel by using starch and agar. However, literature advocates the preparation of different polysaccharide-based mechanically tough hydrogels. Each of these possesses a definite amount of swelling ability. During swelling, hydrogels expand their 3D network, and thus, most of them suffer from a swelling-induced decline in mechanical properties [43]. Moreover, several hydrogels after equilibrium absorption are unable to retain their structural integrity, and this leads to serious performance issues. Although extensive studies have reported various hydrogels with different swelling abilities, only a few of them have reported a retention of mechanical properties both before and after swelling. This may be due to the fact that most of them are too weak after swelling. However, a few studies have reported that hydrogels show noticeable mechanical strength after swelling, for example, Itagaki et al. reported a poly(2-acrylamido-2-methylpropanesulfonic)/polyacrylamide-based hydrogel with retention of mechanical strength after swelling [44]. Similarly, Wang et al. synthesized a poly(*N*-isopropylacrylamide) and a LAPONITEs-based nanocomposite with noticeable mechanical strength after swelling [45]. Although these hydrogels can

retain the mechanical strength after swelling, their applicability is limited due to the use of synthetic monomers. Thus, designing a bio-based hydrogel with strong mechanical attributes, both in the dry and swollen states, is still a big challenge. Hence, in this study, we aimed to produce a mechanically tough polysaccharide-based hydrogel with retention of its swelling-induced mechanical properties. To cross-link the polysaccharides starch and agar, epichlorohydrin (ECH) was used as a cross-linker and different compositions of the hydrogels with varying mechanical performances were prepared. The antibacterial drug ciprofloxacin was encapsulated within the hydrogel and the antibacterial efficiency of the drug-loaded hydrogel was tested against Gram-positive bacteria. Moreover, the controlled release attributes of the hydrogel were investigated in vitro to understand the release profile for the sustained release of drug. Most importantly, to examine the toxicity of the hydrogel towards mammalian cells, cell viability tests were also conducted.

6B.2. Experimental

6B.2.1. Materials

Chemicals such as starch, Luria-Bertani broth, bacterial strains (SA, BS), SDS, LB, crystal violet, and MTT were procured from Himedia, India. Dulbecco's modified Eagle's medium, non-essential amino acids, penicillin-streptomycin solution, L-glutamine, foetal bovine serum, and 4-(2- hydroxyethyl)-1-piperazineethanesulfonic acid were same specifications as described in the **sub-chapter 6A** in section **6A.2.1**.

Agar powder was obtained from Himedia and used to prepare the main backbone of the hydrogel. It is a pale-yellow color polysaccharide with unique gel forming ability.

ECH and sodium hydroxide (NaOH) were used as same specification and same grade as described in **Chapter 3** in **3A.2.1**.

Pohsphosphate-buffered saline (PBS) was purchased from Himedia, India. Before the analysis it was dissolved in distilled water and used in drug release study.

6B.2.2. Methods

6B.2.2.1. Synthesis of the starch-agar-based hydrogel

The starch/agar-based mechanically tough hydrogel was synthesized via a facile one-pot procedure. Calculated amounts of starch and agar powder were placed in a round-bottom flask with distilled water. The reaction temperature was gradually increased under

stirring up to 70–80 ℃ to dissolve both the polysaccharides. Thereafter, the temperature of the reaction mass was lowered to 60 ℃ and at that temperature, the desired amount (0.7185 g) of ECH was added drop wise with the subsequent addition of 3N NaOH solution. The reaction mixture was stirred until all the NaOH had reacted with the ECH as indicated by the increase in the viscosity of the reaction mixture. The viscous gel was then poured onto a Teflon sheet and dried in an oven at 50 ℃ until a touch-free film of the hydrogel formed. Materials with different molar ratios of starch and agar were prepared and encoded as SAC1, SAC2, and SAC3, as tabulated in **Table 6B.1**.

Table 6B.1. Amount of reactants used in formation of the hydrogel

Sample code	Starch content (g)	Agar content (g)	ECH content (g)
SAC1	1.4	0.1	0.7185 g
SAC2	1.2	0.3	0.7185 g
SAC3	1	0.5	0.7185 g

6B.2.3. Structural analysis

The structure of the synthesized starch/agar hydrogel was analyzed by using the same FTIR instrument under similar conditions as described in **Chapter 2**.

6B.2.4. Thermal study

The thermal study of the synthesized hydrogels was done in the same instrument under similar conditions as described in **Chapter 2**.

6B.2.5. Mechanical study

The tensile measurements of the prepared hydrogels were performed using the same Universal Testing Machine (UTM), as described in **Chapter 4**, at a crosshead speed of 5 mm min^{-1}.

6B.2.6. Swelling study

The swelling study of the synthesized hydrogels was done in PBS solution. To determine the swelling ability similar method and mathematical equation were used as described **Chapter 2.**

6B.2.7. Water vapor transmission rate (WVTR)

The WVTR of the SAC3 hydrogel was evaluated following ASTM standard E96-00 with slight modification [46]. A salt solution of calcium chloride and sodium chloride with 2.5 mmol L^{-1} calcium ions and 142 mmol L^{-1} sodium ions (equivalent to the chemical composition of wound fluid and serum) was taken up in a glass vial. The mouth of the vial was covered with hydrogel film, ensuring contact with the water present inside the vial. The mouth of the vial was closed using a Teflon tap so that the vapor could escape only through the hydrogel film. Thereafter, the vial was sealed with the test sample incubated at 37 ℃ temperature, and the weight of the container was measured at regular time intervals (6, 12, 18, 24 h) and an average of three consecutive test results was taken. The equation used to evaluate the WVTR of SAC3 was as follows:

$$\mathbf{WVTR = (m/t)\ 24/A\ (g\ m^{-2}d^{-1})} \text{ ---------- } \mathbf{Eq.\ 6B.1}$$

where m = the mass of water loss after a particular time interval (g), t = time interval (h), and A = the effective transfer area of the hydrogel (m^2) [47].

6B.2.8. Drug loading

Before encapsulation, different amounts of drug were dissolved in distilled water and mixed with the produced gel after the completion of the reaction. Thereafter, the drug-loaded gel was dried in an oven at 50 ℃ until the formation of a touch-free film. To determine the encapsulation efficiency similar method and mathematical equations are used as discussed in **Chapter 6A.**

The percent of drug loading was determined with the help of the following equation [9].

$$\mathbf{Ciprofloxacin\ loading\ (\%) = (weight\ of\ drug\ in\ the\ hydrogel/\ weight\ of\ the\ hydrogel) \times 100} \text{ ----------} \mathbf{Eq.\ 6B.2}$$

6B.2.9. In vitro drug release study

For in vitro release study, the ciprofloxacin loaded hydrogel films were placed in a definite amount of PBS solution at 37 ℃. After predetermined time intervals, 1 mL of drug release buffer was collected. After diluting the drug release buffer by an appropriate amount, the absorbance of the released drug was evaluated by using a UV-vis

spectrophotometer at the λmax (270 nm) of ciprofloxacin. To determine the cumulative release similar mathematical equations are used as described in **Chapter 6A**.

6B.2.10. Antimicrobial testing of the drug loaded hydrogel

The antibacterial study of the drug loaded SAC3 was conducted by using similar method and experimental condition as described in **Chapter 6A.**

6B.2.11. Cytotoxicity studies of the hydrogel on human embryonic kidney cells (HEK 293)

The cytotoxicity studies of the hydrogel of the hydrogels were conducted by using human embryonic kidney cells (HEK 293). This experiment was also conducted similarly as described in **Chapter 6A**.

6B.2.12. Biodegradation via the soil burial

To investigate biodegradation of the synthesized hydrogel soil burial method was used as described in sub-**Chapter 6A**.

6B.3. Results and discussion

6B.3.1. Synthesis of the hydrogel

The possible synthetic pathway for the starch/agar-based mechanically tough hydrogel is demonstrated in **Scheme 6B.1**. In a basic environment, the epoxy rings of ECH were opened and reacted with one of the primary hydroxyl groups of the starch molecules. Consequently, another primary hydroxyl group of starch reacted with the other side of the opened-up epoxy ring of ECH. Moreover, the opened epoxy ring can also react with the primary hydroxyl groups of agar and starch simultaneously, and, thus, the starch/agar cross-linked hydrogel was formed, as depicted in **Scheme 6B.1**.

6B.3.2. FTIR study

The characterization of the synthesized hydrogel was done using FTIR spectroscopy. The FTIR spectra of starch, agar, and all the hydrogels are shown in **Figure 6B.1.**(**a** and **b**). The spectra clearly provide evidence for the ECH cross-linking with the polysaccharides. The absence of an epoxy peak at around 853.88 cm^{-1} and the C–Cl peak at 758.83 cm^{-1} in the spectra of the resulting hydrogels provides evidence for the opening

of the epoxy ring of ECH [48, 15].

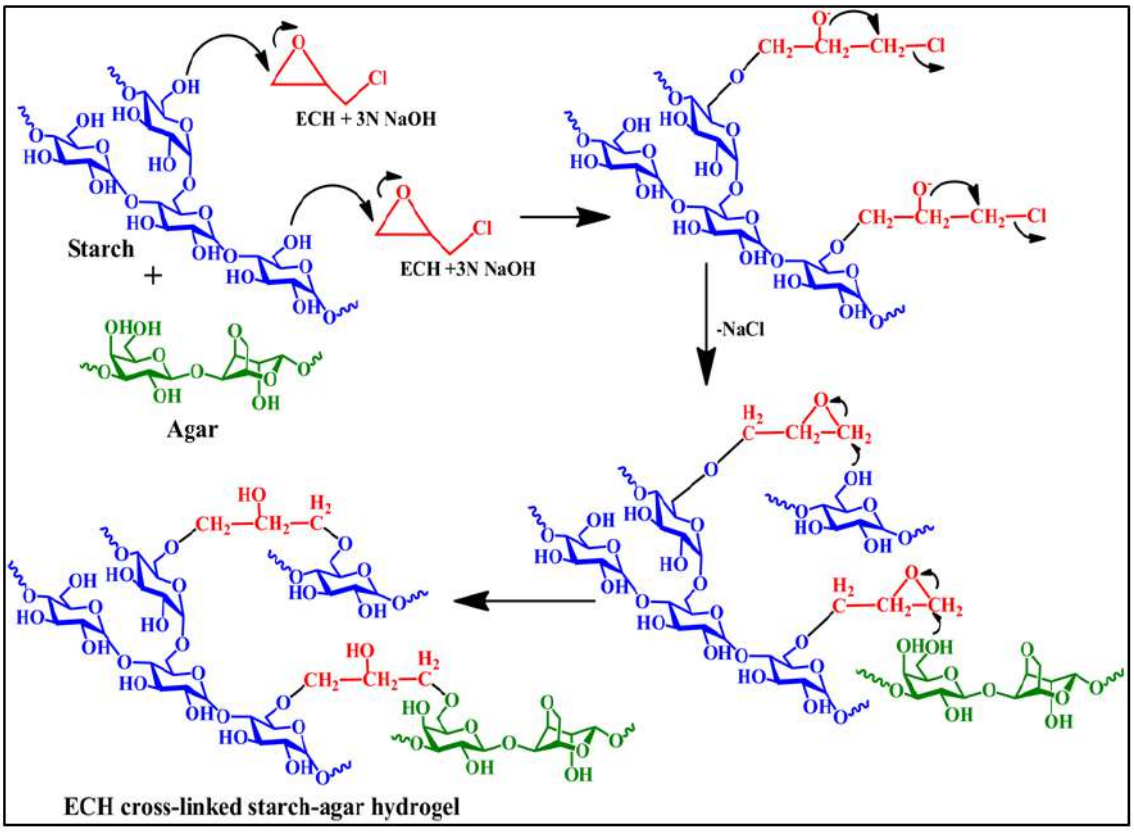

Scheme 6B.1. Possible reaction mechanism for the preparation of the hydrogel.

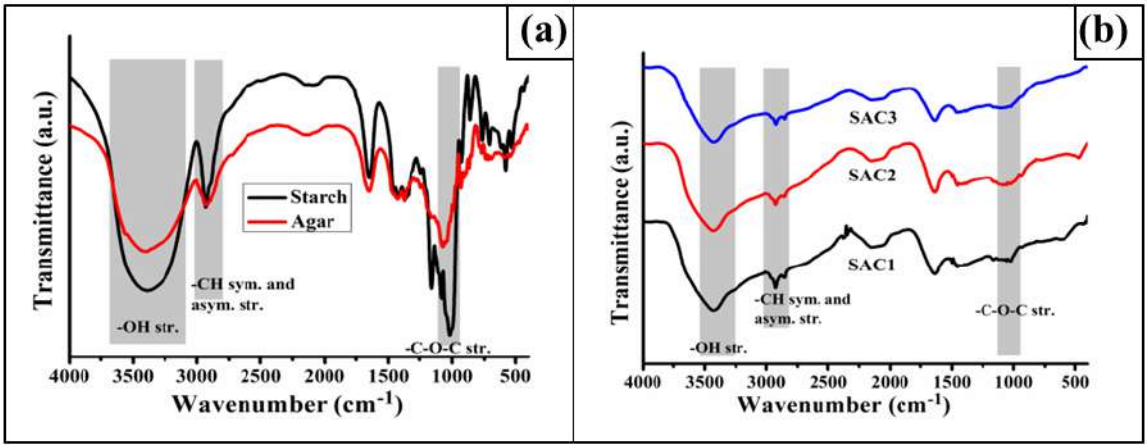

Figure 6B.1. FTIR spectra of (a) agar and starch; (b) SAC1, SAC2, and SAC3.

This observation was also found in our previous work (**Chapter 3** and **4**). In addition to this, the decrease in the broadness of the –OH stretching frequency at 3300–3525 cm^{-1} in the spectra of the synthesized hydrogels revealed the decrease in the degree of free hydroxyl groups in the polysaccharides after ECH cross-linking [49]. All three

compositions of the hydrogels exhibited an –OH stretching frequency at this wavelength range. The characteristic bands for the –CH symmetric and asymmetric stretching frequencies in the range of 2848.15–2976.05 cm^{-1} were present in both the bare polysaccharides and the resulting hydrogel [22]. Moreover, the characteristic band in the range of 1015.42 cm^{-1}–1166.65 cm^{-1} represents the –C–O–C– stretching frequency of both the starch and agar of the resulting hydrogel.

6B.3.3. Thermal study

The TGA thermograms and their first derivatives obtained from the thermal studies of the pristine agar and all three compositions of the hydrogels are shown in **Figure 6B.2.**(**a** and **b**).

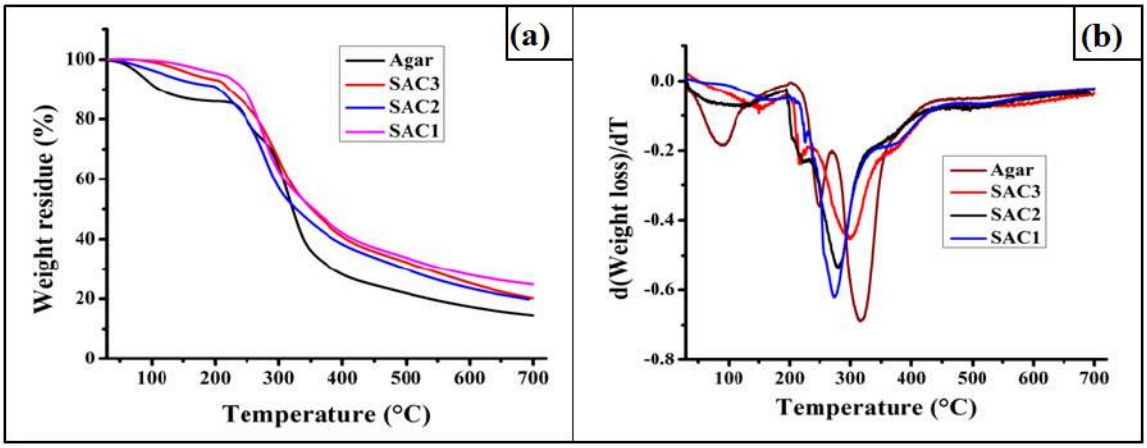

Figure 6B.2. (a) TGA thermograms of agar, SAC1, SAC2, and SAC3; and (b) first derivative TG (DTG) of agar, SAC1, SAC2, and SAC3.

Both the pristine agar and starch–agar films exhibited multistep degradation patterns during thermal decomposition. The first weight loss is due to the loss of moisture entrapped within the agar powder and the hydrogel matrices. In the case of bare agar, in addition to the weight loss due to water vapor, two weight losses were observed at around 248 °C and 316 °C. These two weight losses were also observed for the synthesized hydrogels. However, the degradation pattern observed at 248 °C for the agar backbone was slightly shifted to 219 °C. However, the intensity of this degradation pattern was much lower for SAC1 compared to SAC3, reflecting the lower agar content in the structure. In addition to this, the degradation pattern observed at around 316.23 °C is due to the decomposition of both the bare starch and bare agar backbones, which were also observed for all three hydrogels with some shifting towards lower temperatures [22,

50]. Thus, from this study, it was found that, compared with the bare polysaccharides; the hydrogel films show slightly lower thermal stability.

6B.3.4. Swelling study

Swelling is one of the most important properties of hydrogel for wound dressing, as it provides a moist environment for the wounded tissue. A hydrogel with a balanced swelling ability can cool down the wounded area and provide a comparatively comfortable environment to the host. Moreover, the hydrogel can absorb the exudates from the wound site, which is one of the most important properties for successful wound healing. The effluence from the wound enhanced the probability of bacterial colonization and thus delayed the healing process [51]. The developed hydrogel exhibited a swelling ratio of 2.53±0.45 g g^{-1}-6.167±0.40 gg^{-1} in PBS, as shown in **Figure 6B.3.a.**The hydrogel with a higher starch amount exhibited higher swelling ability. Moreover, an increase in the amount of agar effectively decreased the water absorption capacity. This phenomenon occurs due to the lower hydrophilicity of agar compared to starch as a result of the presence of fewer hydroxyl groups.

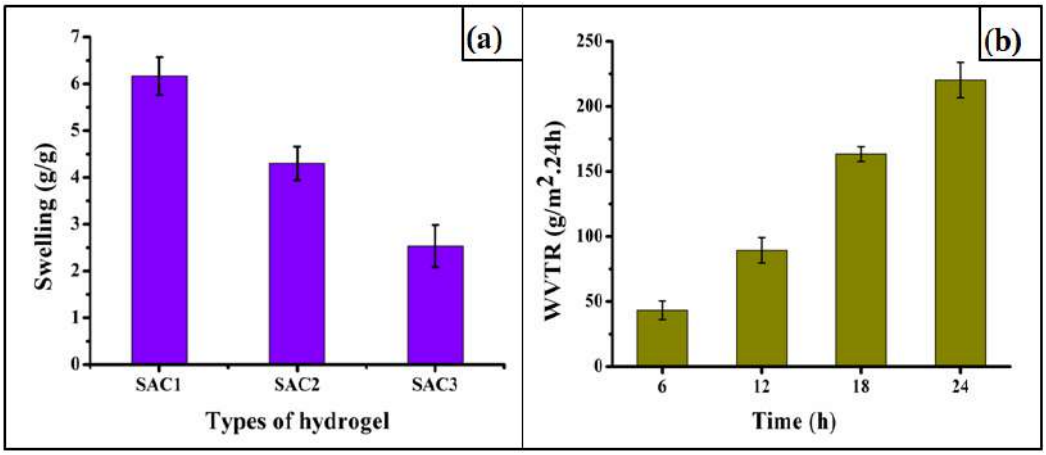

Figure 6B.3. (a) Swelling of the hydrogels and (b) the water transmission rate of SAC3.

6B.3.5. Water vapor transmission rate (WVTR)

Wound healing is a complicated pathophysiological process that requires a suitable moist environment for effective healing. The injured cell exhibits around twenty times higher water loss than normal skin. It has been reported that healing under suitable moist conditions is faster than under dry conditions. Thus, a suitable dressing material is essential for controlling the water evaporation from the wounded area. The WVTR of the

SAC3 hydrogel film over 24 h is shown in **Figure 6B.3.b**. It can be observed that, even if the liquid is in contact with the hydrogel, less water is evaporated, which confirms the synthesized hydrogel to be an effective dressing material.

6B.3.6. Mechanical properties

In the biomedical field, acute wounds on body parts such as knees, fingers, feet, and wrists are difficult to treat due to their frequent movements. Therefore, it is highly recommended that the dressing materials to be used for such specific sites should have adequate mechanical strength. Thus, in this work, a mechanically tough hydrogel was prepared to achieve the required mechanical properties for dressing applications. Taking advantage of the cross-linking of both starch and agar moieties by ECH, the synthesized hydrogel films attained excellent mechanical strength. The typical stress–strain profiles for all three compositions of the hydrogel are shown in **Figure 6B.4.a**. The tensile strength of SAC1 was measured as 9.49±1.29 MPa. In contrast, the stresses of SAC2 and SAC3 were measured as 6.99±0.29 MPa and 6.16±0.37 MPa. Thus, compared to SAC1, the difference between SAC2 and SAC3 is small. These results suggest that the incorporation of agar into the ECH cross-linked starch network affects the mechanical strength of the gels. This may be due to the incorporation of agar resulting in less cross-linking, which may lead to the lower mechanical strength of the hydrogels. Moreover, there are possibilities of starch–starch, and agar–starch cross-linking with the opened-up epoxy ring of ECH. Thus, the penetration of both networks together reduced the tensile strength of the resulting hydrogel. However, the difference was not very pronounced in the case of SAC2 and SAC3 in the dry state.

Further, to provide supportive information for the mechanical strength of the gel, various digital photographs were taken, as shown in **Figure 6B.4.**(**b** and **c**). It can be observed from **Figure 6B.4.b** that the SAC3 hydrogel can be easily bent without any deformation, which provides support for the prominent mechanical strength of the gel. Further, the mechanical strength of the hydrogel was also evaluated by lifting a plastic bottle filled with water with a weight of 135 g using a strip of the hydrogel. It can be seen from **Figure 6B.4.c** that only 0.1 g of hydrogel can lift almost 135 g of weight without any breakage.

Thus, all these results provide supportive information for the mechanical toughness of the synthesized hydrogel. Moreover, the synthesized hydrogel is also transparent enough

for visual inspection of the wound through the hydrogel film without removing it, as shown in **Figure 6B.4.d**.

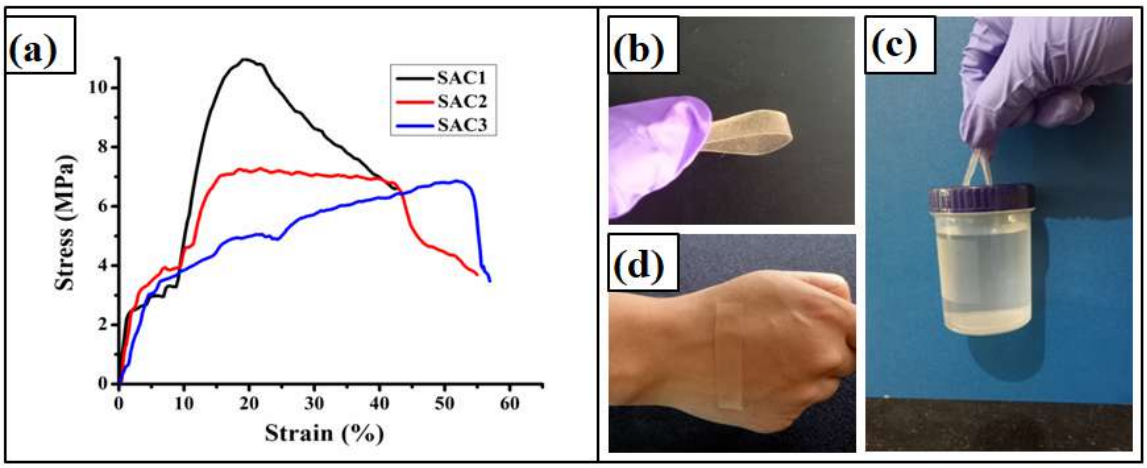

Figure 6B.4. (a) Stress–strain curves of the hydrogels, (b) bending of the hydrogel, (c) weight lifting, and (d) visual inspection of the skin through the hydrogel film.

6B.3.6.1. Mechanical strength after swelling

Along with the high mechanical strength under dry conditions, the synthesized hydrogel can retain its integrity in the swollen state and possess a noticeable amount of tensile strength both in the fully swollen state and with around 70% absorbed water. However, the SAC1 hydrogel possessing the lowest agar content was not suitable for carrying out the mechanical strength testing by the UTM machine. The stress–strain curves for the swollen hydrogels are shown in **Figure 6B.5.**(**a** and **b**). From this figure, it can be clearly observed that SAC3 exhibited a higher tensile strength than SAC2 in both cases. Thus, the noticeable amount of mechanical stability is due to the presence of agar and this property makes the hydrogel suitable for use in dressing applications. To support this fact, gelatinized agar was dried in an oven to a constant weight and kept in water. It can be observed that the dried agar retains its integrity even after 7 days in water, as shown in **Figure 6B.5.**(**c** and **d**). Thus, the presence of agar is responsible for the retention of mechanical strength after swelling, which is also predicted from the tensile strength of the swollen gel. However, in the case of the fully swollen state, much lower tensile strength was observed than in the 70% swollen state, as expected.

The digital photographs of all three compositions of the hydrogels after water absorption are shown in **Figure 6B.5.e**. Moreover, the SAC3 hydrogel in the swollen state can also bend or twist or form a knot, as shown in **Figure 6B.5.**(**f** and **g**).

Thus, all these results prove that the hydrogels have a considerable amount of mechanical strength in the swollen state and that this property arises due to the presence of agar in the network. However, a significant decline in mechanical strength was observed after the absorption of water. This may be due to enhancement in the volume of the hydrogel network by the absorbed water resulting in a lowering of the gel strength. In addition, the hydrophilic groups combined with the water molecules result in decrease of the interactions between the molecular chains present in the hydrogel [52].

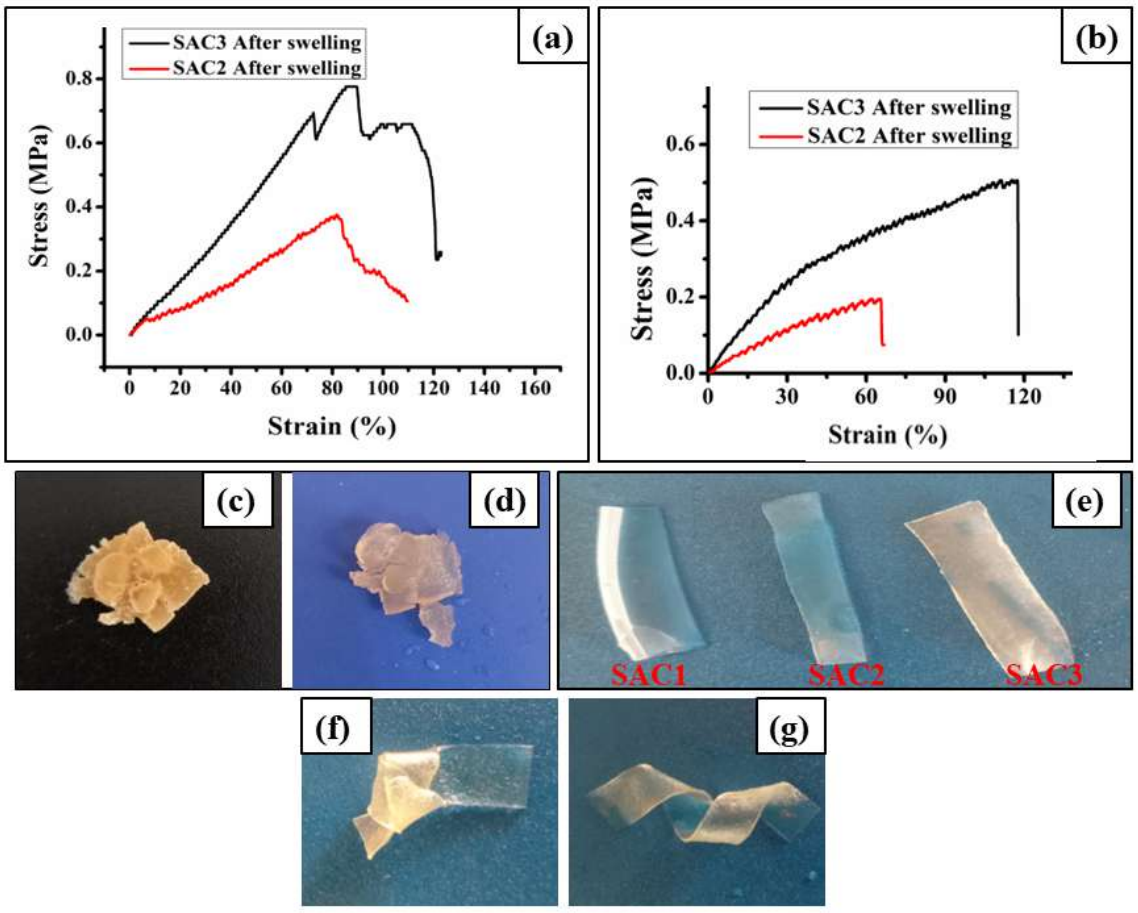

Figure 6B.5. Mechanical strength of the three compositions of the hydrogel after swelling (a) at 70% water absorption and (b) in the fully swollen state; (c) dried agar gel, (d) swollen agar gel after 7 days swelling in water, (e) digital photographs of the three compositions of the gel after swelling, (f) knot formation of the swollen gel, and (g) bending of the swollen gel.

6B.3.7. Drug loading and encapsulation efficiency

In a controlled drug delivery system, drug loading and encapsulation efficiencies are the most important parameters. **Figure 6B.6.a** shows the drug loading and encapsulation efficiencies of the SAC3 hydrogel with different weight percentages of ciprofloxacin.

The loading amount of the drug significantly affected the encapsulation efficiency of the hydrogel, and the highest encapsulation efficiency was observed in the case of 10% loading. However, the encapsulation efficiency of the hydrogel decreased upon an increase in the amount of the loaded drug. This result indicates that, with an increase in the amount of drug loaded in the hydrogel, a greater percentage of the drug was lost during encapsulation [53].

6B.3.8. Drug release

The drug loading efficiency also affected the controlled release ability of the hydrogel, as shown in **Figure 6B.6.(b** and **c)**.

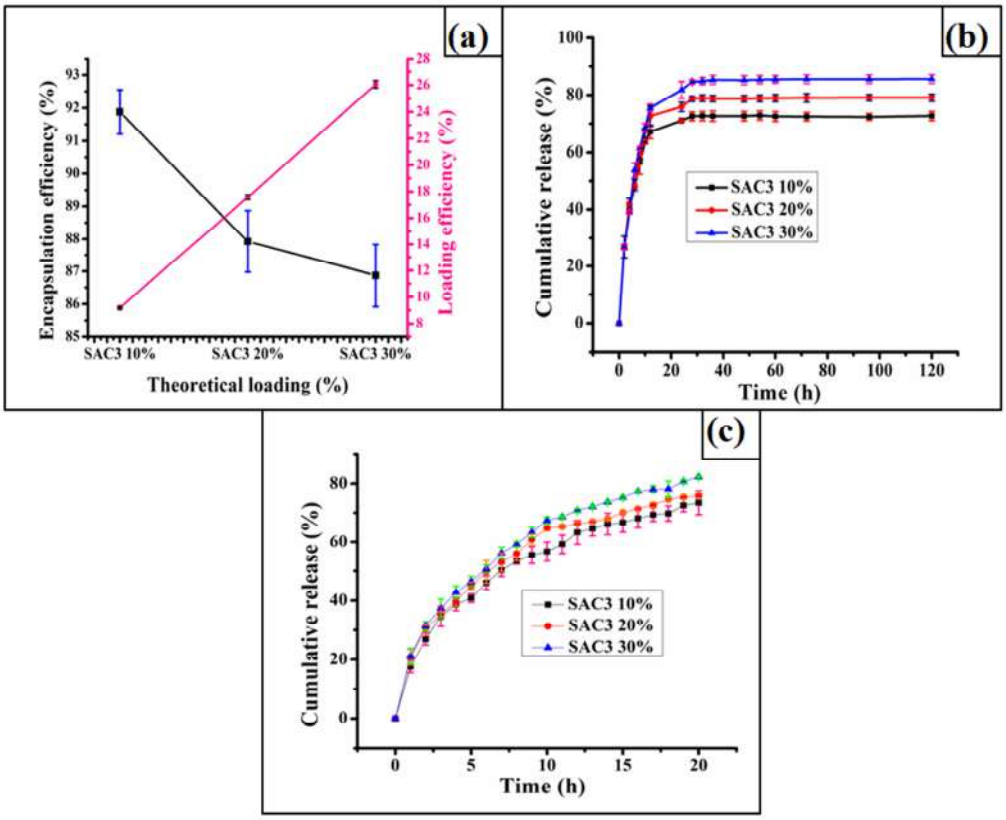

Figure 6B.6. (a) Drug encapsulation and loading efficiency; cumulative drug release profile over (b) 120 h and (c) 20 h.

It was examined that the percentage releasing ability of hydrogel increased with the increase in loading amount and SAC3 with 30% loading showed the highest percentage of release, followed by 20% and 10% loading. This increase in the release amount is mainly due to a diffusion-controlled phenomenon, as the extent of swelling in all the cases was the same. Thus, with the increase in the drug loading, the rate of diffusion

enhanced with the increase in the concentration gradient [54]. In the case of a swellable system, liquid molecules penetrate inside the hydrogel matrix and the drug molecules encapsulated inside the network come out due to Brownian movement. The encapsulated ciprofloxacin exhibited sustained release in all the three cases; a property that is one of the most important characteristics for the successful healing of any affected wound. Initially, the drug release rate from the hydrogel was much higher, but the release rate decreased gradually with time, and after 28 h the drug release rate almost reached equilibrium, as shown in **Figure 6B.6.b**. Moreover, we also studied the drug release rate over 1 h interval to investigate the effect of loading amount, as shown in **Figure 6B.6.c**.

To investigate the drug release mechanism various mathematical models are used as shown in **Figure 6B.7.**

Similar to sub-**Chapter 6A**, non-Fickian drug release was obtained from Korsmeyer and Peppas power law models. Moreover, the kinetics data obtained from the various models such as zero order, pseudo first order, and Higuchi square root law are shown in **Table 6B.2.**

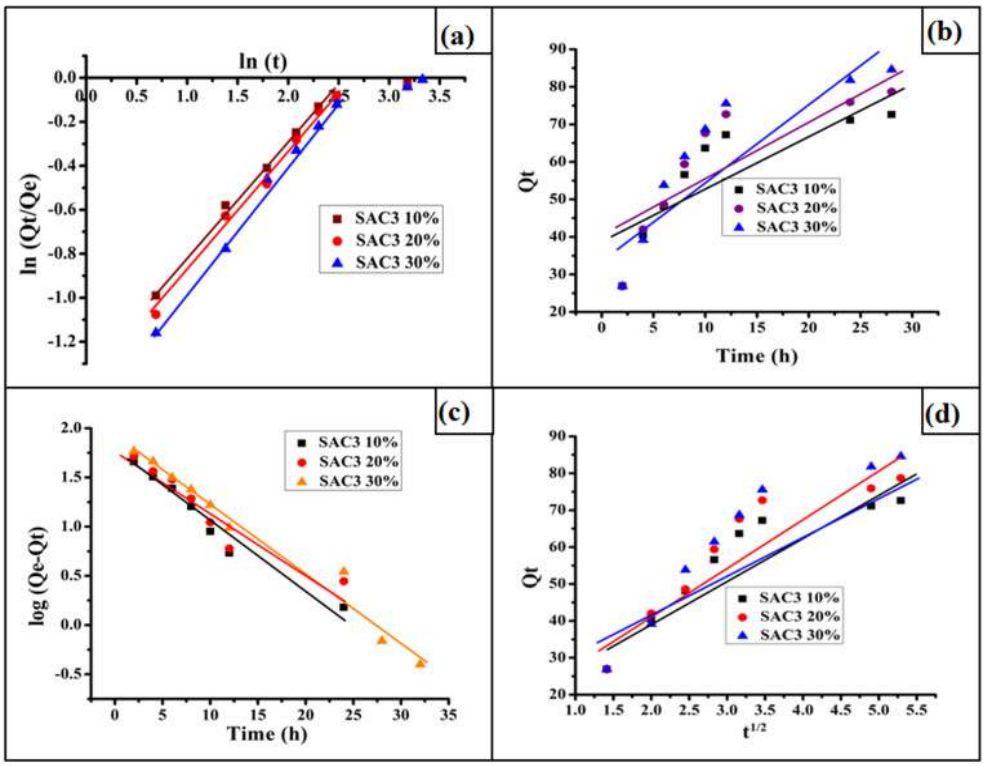

Figure 6B.7. (a) Korsmeyer and Peppas power law, (b) zero order kinetics, (c) pseudo first-order kinetics, and (d) Higuchi square root law at different loadings.

Table 6B.2. Kinetics parameters for drug release systems

Drug release systems	Korsmeyer and Peppas power law		Zero-order (R^2)	Pseudo-first-order (R^2)	Higuchi square root law (R^2)
	(R^2)	n value			
SAC3 30%	0.9940	0.59	0.7068	0.9720	0.8523
SAC3 20%	0.9923	0.55	0.6594	0.8935	0.8134
SAC3 10%	0.9944	0.51	0.6476	0.9539	0.8066

6B.3.9. Antibacterial activity

After injuries, bacterial infections of the wounded skin are very common and these lead to a delayed healing process and serious tissue damage. Thus, dressing materials should possess a definite amount of antibacterial activity. To investigate the antibacterial activity of the drug-loaded SAC3, the hydrogel without the drug, ciprofloxacin-loaded hydrogel, and ciprofloxacin solution as a control were placed in separate segments of agar plates. After 24 h, the drug-loaded hydrogel effectively exhibited an inhibition effect against the tested bacterial strains. However, the hydrogel samples without drug encapsulation did not show any antibacterial activity. The zones of inhibition for each bacterial strain are shown in **Figure 6B.8.**(**a** and **b**) and the diameters of the inhibition zones are given in **Table 6B.3**.

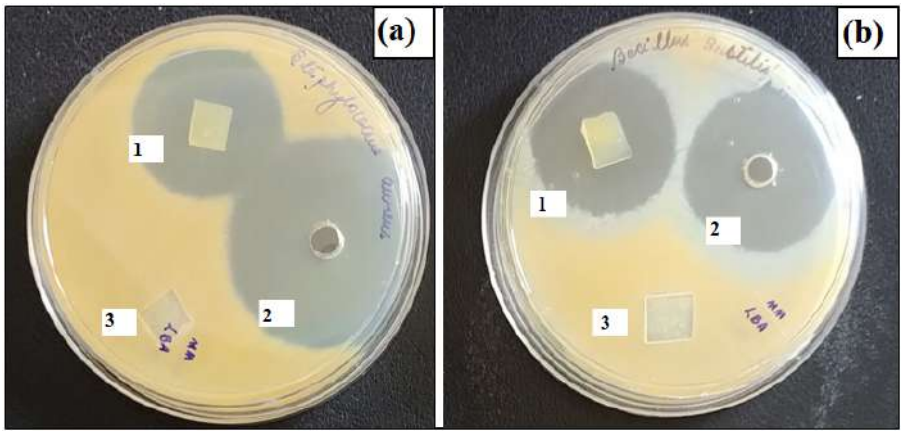

Figure 6B.8. Antibacterial activity of (1) SAC3 with drug, (2) control, and (3) SAC3 without drug: against (a) SA and (b) BS.

These results provide supportive information that the drug was successfully loaded with SAC3 and that after encapsulation the hydrogel exhibits antibacterial activity. Thus, the

in vitro antibacterial studies demonstrated that drug-loaded SAC3 exhibits sustained antibacterial activity against bacterial starins. Hence, the hydrogel can be efficiently used as an antibacterial dressing material for infected wounds.

Table 6B.3. Inhibition zone diameter of the hydrogel

Bacterial strain	Hydrogel with out drug	Drug loaded hydrogel	Control system
BS	0	24±1	33.67±0.58
SA	0	32.67±1.15	40±0

6B.3.10. Biocompatibility testing

Biocompatibility is the most essential property of biomaterials. Favorable cell compatibility is a prerequisite in the design of a biomaterial for wound dressing applications. In this study, to assess biocompatibility, human embryonic kidney cells (HEK 293) were employed against the SAC3 hydrogel without the loading of any drug. Different concentrations of hydrogel samples with this cell type were cultured for 24 h and the results were plotted as shown in **Figure 6B.9.a**.

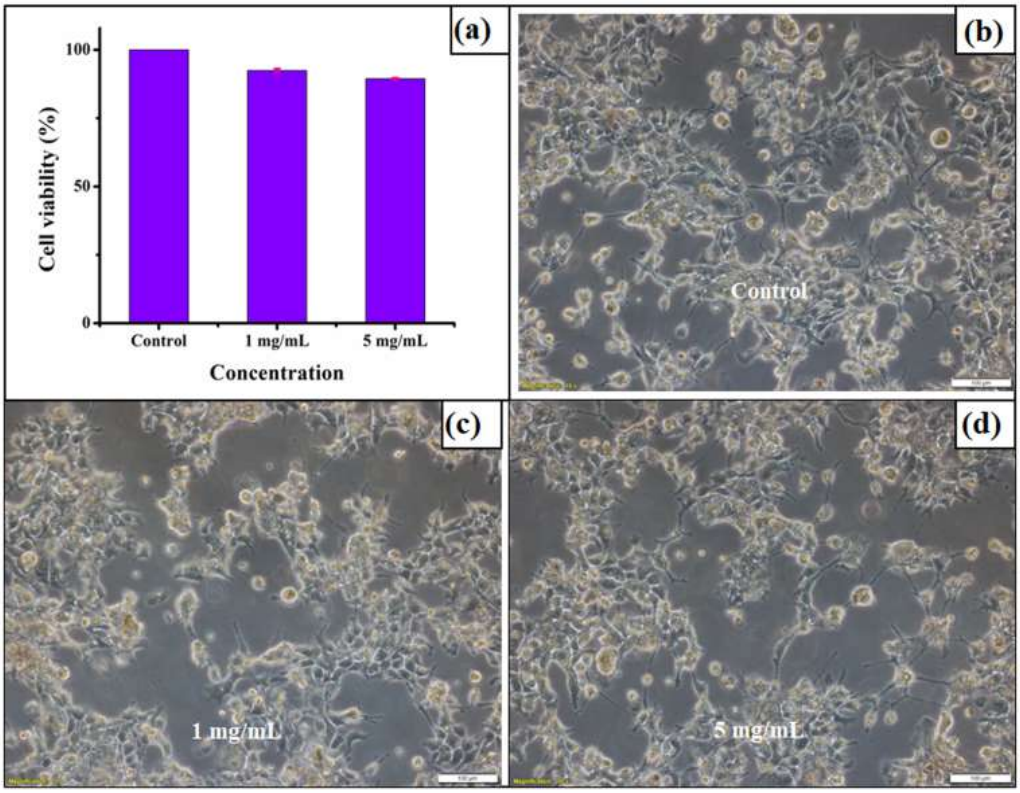

Figure 6B.9. (a) Cell viability of human embryonic kidney cells (HEK 293) with SAC3

hydrogel; microscopy images of the cells (b) without treatment, and treated with (c) 1 mg mL^{-1} SAC3 and (d) 5 mg mL^{-1} SAC3.

The cell viability slightly decreased with the increase in the concentration of the hydrogel, but a minimum 89.46± 0.38% cell viability was obtained. Thus, the hydrogel exhibited an acceptable range of cell viability, suggesting that the synthesized hydrogel is non-toxic and can be safely employed as a dressing material for wound healing. Moreover, after treatment with different concentrations of SAC3, the change in cell morphology was also studied with the help of an inverted microscope, as shown in **Figure 6B.9.b-d**. The cell morphology remained intact after treatment and only a slight difference was observed, indicating the biocompatible nature of the synthesized hydrogel.

6B.3.11. Biodegradation

Biodegradation of a polymeric material is an essential property from an environmental point of view. In most of the cases, dressing materials are removed regularly after certain time intervals and the non-degradability of these can cause serious environmental pollution. Thus, we studied the biodegradation of the synthesized hydrogel. It was seen that the hydrogel was easily degraded by up to 92.33±2.52% within one month when it was buried under the soil (**Figure 6B.10.a**) at our university campus.

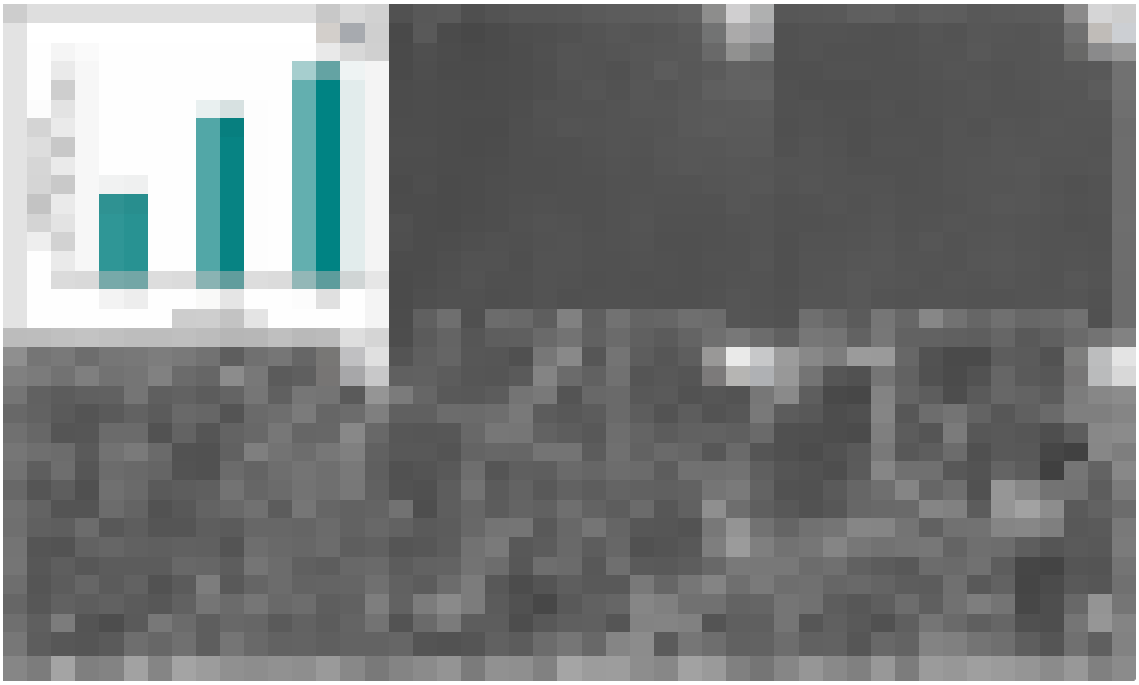

Figure 6B.10. (a) Weight loss of SAC3 after degradation at various time intervals, (b

and c) SEM images of the SAC3 before biodegradation, and (d–f) SEM images of SAC3 after degradation.

The micro-organisms present in the soil are responsible for this degradation [39] and the degradation was enhanced due to the absence of synthetic monomers. The SEM images of the oven-dried hydrogel films before and after degradation are shown in **Figure 6B.10.b-f**. It is seen that the smooth surface of the hydrogel became rough due to the erosion caused by the degradation. Thus, the SEM images provide the supportive information for the biodegradation of the synthesized hydrogels.

6B.4. Conclusion

In summary, a mechanically tough polysaccharide-based hydrogel was developed without the inclusion of any synthetic monomers. The synthesized hydrogel possesses outstanding mechanical strength (9.49±1.29–6.16±0.37 MPa), making it suitable for wound dressing applications. Moreover, the hydrogel can retain its integrity in the swollen state too, and incredible tensile strength was obtained under such conditions. This property aids the easy removal of the dressing material, meaning that it might be less painful to the host. In addition, the hydrogel exhibits a controlled water transmission rate, which is one of the most important properties of a dressing material. Moreover, the drug-loaded hydrogel exhibited efficient antibacterial activity against the tested bacterial strains. The hydrogels without any drugs also showed good biocompatibility with human embryonic kidney cells (HEK 293) and minimum 89.46±0.38% cell viability was observed. Above all, the hydrogels exhibit a minimum 86.87±0.95% encapsulation efficiency of the drug with maximum 85.28±1.58% sustained release ability. Thus, this work details the preparation of a mechanically strong, bio-based, biocompatible hydrogel, which exhibits antibacterial drug release ability upon drug loading and hence can be used as a wound dressing. In conclusion, this work shows promise for the development of polysaccharide-based dressing materials.

References

[1] Dai, L., Zhang, L., Wang, B., Yang, B., Khan, I., Khan, A., and Ni, Y. Multifunctional self-assembling hydrogel from guar gum. *Chemical Engineering Journal*, 330:1044-1051, 2017.

[2] Alam, M. N. and Christopher, L. P. Natural cellulose-chitosan cross-linked superabsorbent hydrogels with superior swelling properties. *ACS Sustainable*

Chemistry & Engineering, 6:8736-8742, 2018.

[3] Kamoun, E. A. N-succinyl chitosan–dialdehyde starch hybrid hydrogels for biomedical applications. *Journal of Advanced research*, 7:69-77, 2016.

[4] Guo, J., Ge, L., Li, X., Mu, C., and Li, D. Periodate oxidation of xanthan gum and its crosslinking effects on gelatin-based edible films. *Food Hydrocolloids*, 39:243-250, 2014.

[5] Fan, L. H., Pan, X. R., Zhou, Y., Chen, L. Y., Xie, W. G., Long, Z. H., and Zheng, H. Preparation and characterization of crosslinked carboxymethyl chitosan–oxidized sodium alginate hydrogels. *Journal of Applied Polymer Science*, 122:2331-2337, 2011.

[6] Zhang, Y., Fu, C., Li, Y., Wang, K., Wang, X., Wei, Y., and Tao, L. Synthesis of an injectable, self-healable and dual responsive hydrogel for drug delivery and 3D cell cultivation. *Polymer Chemistry*, 8:537-544, 2017.

[7] Li, S., Pei, M., Wan, T., Yang, H., Gu, S., Tao, Y., and Xiao, P. Self-healing hyaluronic acid hydrogels based on dynamic Schiff base linkages as biomaterials. *Carbohydrate polymers*, 250:116922, 2020.

[8] Saxena, A., Sachin, K., Bohidar, H. B., and Verma, A. K. Effect of molecular weight heterogeneity on drug encapsulation efficiency of gelatin nano-particles. *Colloids and Surfaces B: Biointerfaces*, 45:42-48, 2005.

[9] Heydari, A., Pardakhti, A., and Sheibani, H. Preparation and characterization of zwitterionic poly (β-cyclodextrin-co-guanidinocitrate) hydrogels for ciprofloxacin controlled release. *Macromolecular Materials and Engineering*, 302:1600501, 2017.

[10] Rather, M. A., Deori, P. J., Gupta, K., Daimary, N., Deka, D., Qureshi, A., and Mandal, M. Ecofriendly phytofabrication of silver nanoparticles using aqueous extract of Cuphea carthagenensis and their antioxidant potential and antibacterial activity against clinically important human pathogens. *Chemosphere*, 300: 134497, 2022.

[11] Gupta, K., Barua, S., Hazarika, S. N., Manhar, A. K., Nath, D., Karak, N., and Mandal, M. Green silver nanoparticles: enhanced antimicrobial and antibiofilm activity with effects on DNA replication and cell cytotoxicity. *RSC Advances*, 4:52845-52855, 2014.

[12] Mert, H., Özkahraman, B., and Damar, H. A novel wound dressing material: Pullulan grafted copolymer hydrogel via UV copolymerization and

crosslinking. *Journal of Drug Delivery Science and Technology*, 60:101962, 2020.

[13] Pandit, A. H., Mazumdar, N., and Ahmad, S. Periodate oxidized hyaluronic acid-based hydrogel scaffolds for tissue engineering applications. *International journal of biological macromolecules*, 137:853-869, 2019.

[14] Nypelö, T., Berke, B., Spirk, S., and Sirviö, J. A. Periodate oxidation of wood polysaccharides-Modulation of hierarchies. *Carbohydrate Polymers*, 252: 117105, 2021.

[15] Sarmah, D. and Karak, N. Double network hydrophobic starch based amphoteric hydrogel as an effective adsorbent for both cationic and anionic dyes. *Carbohydrate polymers*, 242:116320, 2020.

[16] Varma, R. and Vasudevan, S. Extraction, characterization, and antimicrobial activity of chitosan from horse mussel modiolus modiolus. *ACS omega*, 5:20224-20230, 2020.

[17] Lustriane, C., Dwivany, F. M., Suendo, V., and Reza, M. Effect of chitosan and chitosan-nanoparticles on post harvest quality of banana fruits. *Journal of Plant Biotechnology*, 45:36-44, 2018.

[18] Tang, J., Javaid, M. U., Pan, C., Yu, G., Berry, R. M., and Tam, K. C. Self-healing stimuli-responsive cellulose nanocrystal hydrogels. *Carbohydrate polymers*, 229:115486, 2020.

[19] Thakur, S., Kumari, S., Dogra, P., and Chauhan, G. S. A new guar gum-based adsorbent for the removal of Hg (II) from its aqueous solutions. *Carbohydrate polymers*, 106:276-282, 2014.

[20] Zhang, M., Song, L., Jiang, H., Li, S., Shao, Y., Yang, J., and Li, J. Biomass based hydrogel as an adsorbent for the fast removal of heavy metal ions from aqueous solutions. *Journal of Materials Chemistry A*, 5(7):3434-3446, 2017.

[21] Perez, J. J. and Francois, N. J. Chitosan-starch beads prepared by ionotropic gelation as potential matrices for controlled release of fertilizers. *Carbohydrate polymers*, 148:134-142, 2016.

[22] Sarmah, D. and Karak, N. Biodegradable superabsorbent hydrogel for water holding in soil and controlled-release fertilizer. *Journal of Applied Polymer Science*, 137(13):48495, 2020.

[23] Jayakumar, R., Nagahama, H., Furuike, T., and Tamura, H. Synthesis of phosphorylated chitosan by novel method and its characterization. *International*

journal of biological macromolecules, 42(4):335-339, 2008.

[24] Nguyen, V. T., Dang, T. B., and Trinh, K. S. Electrolytic oxidation of gelatinised tapioca starch: effect of sodium chloride content on structural and physicochemical properties. *International Food Research Journal*, 28(1):56-62, 2021.

[25] Song, G., Zhao, Z., Peng, X., He, C., Weiss, R. A., and Wang, H. Rheological behavior of tough PVP-in situ-PAAm hydrogels physically cross-linked by cooperative hydrogen bonding. *Macromolecules*, 49(21):8265-8273, 2016.

[26] Su, H., Zheng, R., Jiang, L., Zeng, N., Yu, K., Zhi, Y., and Shan, S. Dextran hydrogels via disulfide-containing Schiff base formation: Synthesis, stimuli-sensitive degradation and release behaviors. *Carbohydrate Polymers*, 265: 118085, 2021.

[27] Azadikhah, F., Karimi, A. R., Yousefi, G. H., and Hadizadeh, M. Dual antioxidant-photosensitizing hydrogel system: Cross-linking of chitosan with tannic acid for enhanced photodynamic efficacy. *International Journal of Biological Macromolecules*, 188:114-125, 2021.

[28] Malik, N. S., Ahmad, M., Minhas, M. U., Tulain, R., Barkat, K., Khalid, I., and Khalid, Q. Chitosan/xanthan gum based hydrogels as potential carrier for an antiviral drug: Fabrication, characterization, and safety evaluation. *Frontiers in Chemistry*, 8:50, 2020.

[29] Peng, Z., Peng, Z., and Shen, Y. Fabrication and properties of gelatin/chitosan composite hydrogel. *Polymer-Plastics Technology and Engineering*, 50(11): 1160-1164, 2011.

[30] Park, H., Park, K., and Kim, D. Preparation and swelling behavior of chitosan-based superporous hydrogels for gastric retention application. *Journal of Biomedical Materials Research Part A,* 76(1):144-150, 2006.

[31] Gull, N., Khan, S. M., Butt, O. M., Islam, A., Shah, A., Jabeen, S., and Butt, M. T. Z. Inflammation targeted chitosan-based hydrogel for controlled release of diclofenac sodium. *International Journal of Biological Macromolecules*, 162: 175-187, 2020.

[32] Kajjari, P. B., Manjeshwar, L. S., and Aminabhavi, T. M. Novel interpenetrating polymer network hydrogel microspheres of chitosan and poly (acrylamide)-grafted-guar gum for controlled release of ciprofloxacin. *Industrial & Engineering Chemistry Research*, 50(23):13280-13287, 2011.

[33] Anirudhan, T. S. and Rejeena, S. R. Poly (acrylic acid-co-acrylamide-co-2-acrylamido-2-methyl-1-propanesulfonic acid)-grafted nanocellulose/poly (vinyl alcohol) composite for the in vitro gastrointestinal release of amoxicillin. *Journal of Applied Polymer Science*, 131:, 2014.

[34] Pathania, D., Verma, C., Negi, P., Tyagi, I., Asif, M., Kumar, N. S., and Gupta, V. K. Novel nanohydrogel based on itaconic acid grafted tragacanth gum for controlled release of ampicillin. *Carbohydrate Polymers*, 196:262-271, 2018.

[35] Sreedharan, S. M. and Singh, R. Ciprofloxacin functionalized biogenic gold nanoflowers as nanoantibiotics against pathogenic bacterial strains. *International Journal of Nanomedicine*, 9905-9916, 2019.

[36] Abbas, A., Hussain, M. A., Amin, M., Tahir, M. N., Jantan, I., Hameed, A., and Bukhari, S. N. A. Multiple cross-linked hydroxypropylcellulose–succinate–salicylate: prodrug design, characterization, stimuli responsive swelling–deswelling and sustained drug release. *RSC Advances*, 5(54):43440-43448, 2015.

[37] Samuelov, Y., Donbrow, M., and Friedman, M. Sustained release of drugs from ethylcellulose-polyethylene glycol films and kinetics of drug release. *Journal of Pharmaceutical Sciences*, 68(3):325-329, 1979.

[38] Hanna, D. H. and Saad, G. R. Encapsulation of ciprofloxacin within modified xanthan gum-chitosan based hydrogel for drug delivery. *Bioorganic Chemistry*, 84:115-124, 2019.

[39] Thombare, N., Mishra, S., Siddiqui, M. Z., Jha, U., Singh, D., and Mahajan, G. R. Design and development of guar gum based novel, superabsorbent and moisture retaining hydrogels for agricultural applications. *Carbohydrate Polymers*, 185:169-178, 2018.

[40] Liu, L., Li, X., Nagao, M., Elias, A. L., Narain, R., and Chung, H. J. A pH-Indicating colorimetric tough hydrogel patch towards applications in a substrate for smart wound dressings. *Polymers*, 9(11):558, 2017.

[41] Fang, K., Wang, R., Zhang, H., Zhou, L., Xu, T., Xiao, Y., and Fu, J. Mechano-responsive, tough, and antibacterial zwitterionic hydrogels with controllable drug release for wound healing applications. *ACS Applied Materials & Interfaces*, 12(47):52307-52318, 2020.

[42] Chen, H., Peng, C., Wang, L., Li, X., Yang, M., Liu, H., and Chen, W. Mechanically tough, healable hydrogels synergistically reinforced by UV-responsive crosslinker and metal coordination interaction for wound healing

application. *Chemical Engineering Journal*, 403:126341, 2021.

[43] Chen, H., Yang, F., Hu, R., Zhang, M., Ren, B., Gong, X., and Zheng, J. A comparative study of the mechanical properties of hybrid double-network hydrogels in swollen and as-prepared states. *Journal of Materials Chemistry B*, 4(35):5814-5824, 2016.

[44] Itagaki, H., Kurokawa, T., Furukawa, H., Nakajima, T., Katsumoto, Y., and Gong, J. P. Water-induced brittle-ductile transition of double network hydrogels. *Macromolecules*, 43(22):9495-9500, 2010.

[45] Wang, T., Liu, D., Lian, C., Zheng, S., Liu, X., and Tong, Z. Large deformation behavior and effective network chain density of swollen poly (N-isopropylacrylamide)–laponite nanocomposite hydrogels. *Soft Matter*, 8(3):774-783, 2012.

[46] Lu, G., Ling, K., Zhao, P., Xu, Z., Deng, C., Zheng, H., and Chen, J. A novel in situ-formed hydrogel wound dressing by the photocross-linking of a chitosan derivative. *Wound Repair and Regeneration*, 18(1):70-79, 2010.

[47] Wu, P., Fisher, A. C., Foo, P. P., Queen, D., and Gaylor, J. D. S. In vitro assessment of water vapour transmission of synthetic wound dressings. *Biomaterials*, 16(3):171-175, 1995.

[48] Song, Y., Li, L., and Zheng, Q. Influence of epichlorohydrin modification on structure and properties of wheat gliadin films. *Journal of Agricultural and Food Chemistry*, 57(6):2295-2301, 2009.

[49] Zhang, L., Zhou, J., and Zhang, L. Structure and properties of β-cyclodextrin/cellulose hydrogels prepared in NaOH/urea aqueous solution. *Carbohydrate Polymers*, 94(1):386-393, 2013.

[50] Roy, S. and Rhim, J. W. Fabrication of pectin/agar blended functional film: Effect of reinforcement of melanin nanoparticles and grapefruit seed extract. *Food Hydrocolloids*, 118:106823, 2021.

[51] He, J., Shi, M., Liang, Y., and Guo, B. Conductive adhesive self-healing nanocomposite hydrogel wound dressing for photothermal therapy of infected full-thickness skin wounds. *Chemical Engineering Journal*, 394:124888, 2020.

[52] Wang, R., Li, N., Jiang, B., Li, J., Hong, W., and Jiao, T. Facile preparation of agar/polyvinyl alcohol-based triple-network composite hydrogels with excellent mechanical performances. *Colloids and Surfaces A: Physicochemical and Engineering Aspects*, 615:126270, 2021.

[53] Wang, S. B., Chen, A. Z., Weng, L. J., Chen, M. Y., and Xie, X. L. Effect of Drug-loading Methods on Drug Load, Encapsulation Efficiency and Release Properties of Alginate/Poly-L-Arginine/Chitosan Ternary Complex Microcapsules. *Macromolecular Bioscience*, 4(1):27-30, 2004.

[54] Yu, C. Y., Zhang, X. C., Zhou, F. Z., Zhang, X. Z., Cheng, S. X., and Zhuo, R. X. Sustained release of antineoplastic drugs from chitosan-reinforced alginate microparticle drug delivery systems. *International Journal of Pharmaceutics*, 357(1-2):15-21, 2008.